

AN ELECTRONIC SIMULATOR FOR THE REPRESENTATION OF
SYNCHRONOUS GENERATORS IN NETWORK ANALYSERS

BY

E.H. GOUWS

Thesis submitted to the
Department of Electrical Engineering
of the University of Cape Town
for the degree of
Doctor of Philosophy

1964

The copyright of this thesis vests in the author. No quotation from it or information derived from it is to be published without full acknowledgement of the source. The thesis is to be used for private study or non-commercial research purposes only.

Published by the University of Cape Town (UCT) in terms of the non-exclusive license granted to UCT by the author.

ACKNOWLEDGMENTS

My sincere thanks are due to:

Col. G.H. Webster and Dr. J.L.N. Besseling, who supervised this thesis.

Mr. L.L. van Zyl, formerly of the Fishing Industries Research Institute for his assistance and advice.

The Electricity Supply Commission, for its encouragement to undertake this research project.

The Staff of the Department of Electrical Engineering, University of Cape Town, for their help.

SUMMARY

The basic principles of the transient behaviour of a generator are briefly explained, and a non-linear differential equation describing the generator's performance is given. The need for a calculating aid for solving this non-linear equation is explained.

An analogue of a generator is derived, and details of a simulator based on this analogue are given. Experimental results are given to show that the simulator behaves according to theory.

Further development of the basic apparatus to increase its accuracy and versatility is described.

C O N T E N T S

1. INTRODUCTION	1
2. PROPERTIES OF AN ALTERNATOR	4
2.1. Internal emf. and reactance.	4
2.2. Inertia and stored energy.	6
2.3. Dynamic equation of the machine.	7
3. THE SIMULATION OF A SYNCHRONOUS GENERATOR.	9
3.1. Derivation of the analogue representation.	9
3.2. Scaling of the analogue simulator.	15
3.3. Derivation of the analogue with damping included.	19
3.4. Scaling the generator, including damping effects.	21
4. EXPERIMENTAL RESULTS.	23
4.1. Steady-state test.	23
4.2. Transient stability study.	25
4.2.1. Transient stability - Study 1.	25
4.2.2. Transient stability - Study 2.	30
4.3. Integrator transient test.	33
5. CONCLUSIONS.	35
APPENDICES	
A. Generator damping power	A1
B. The phase detector.	B1

C. 1. Gain of the differential operational amplifier.	C1
2. The damped integrator.	C2
D. Alternator damping coefficient.	D1
1. Study 1.	D1
2. Study 2.	D3
E. Specifications and circuit diagrams.	E1
1. D.C. amplifiers	E1
2. A.C. units	E5
(i) Variable frequency oscillator.	E5
(ii) Low-pass filter and pre-amplifier	E6
(iii) Power amplifier	E8
(iv) Phase detector	E9
F. Auxilliary equipment.	F1
1. Phase angle recorder	F1
2. Network impedance switching unit.	F2

REFERENCES.

1. INTRODUCTION

Modern developments in materials and techniques have made it possible to increase the power rating of generators by an order of magnitude compared with the average machine of a decade ago. This has resulted in higher power outputs from machines whose physical size is severely limited by factors such as transportation of the generator parts from factory to final site. Because of this, modern alternators have much lower inertia constants, which adversely affect their transient-stability characteristics.^{1, 2.}

The increase in electrical loading has resulted in transient reactances that are higher than before, which also causes generators to be less stable under transient conditions.^{3.}

The trend is to build power stations at sites where their fuel can be had cheaply, and to transmit the generated power over long distances to the places where the power is used. With the rising demand, more power must be generated, and more generators have to be connected to the power distribution system. Long transmission lines increase the likelihood of system oscillations. Since generators are run very close to their stability limit for reasons of economy, loss of synchronism can happen very easily.

The calculation of the effects of faults, sudden load changes and other disturbances has become very necessary, to ensure that the supply of electric power to the consumers takes place without interruption and with the highest possible economy. Where systems are small these calculations

present.....

present little difficulty, but they become very tedious as the complexity of the system is increased, so that some tool to ease the problem is necessary.

A computing aid is also almost essential for the designer when planning a system. With this he can select optimum values for the various units in his design.

Network analysers have long been used to solve steady state problems, but doing transient calculations the work becomes involved, especially if it is a multi-machine problem. In recent years the shortcomings of the simple network analyser have caused new techniques to be evolved to overcome these limitations. A more exact representation of the transient behaviour of a generator was required. Some of the methods used are:

- Micro-machines 4, 5, 6
- Electro-mechanical models 7, 8, 9
- Digital computers 10,11, 12
- Analogue computers 13, 14, 15, 16, 17, 18, 19
- Hybrid simulators 20, 21, 22, 23, 24, 25

The relative merits of the various methods have been discussed. ^{26.}
It would seem as if an analogue solution of machine equations holds the greatest promise. Hybrid simulators, making use of analogue techniques as well as a.c. network analyser methods are more attractive than general purpose analogue computers, since they allow steady state computations such as fault current and load flow calculations to be made in addition to the

investigations.....

investigation of transient problems, with a great saving in computing equipment, especially where asymmetrical faults are applied.^{23.}

The choice of the type of calculating aid to be built for this thesis project was also influenced by the fact that a small a.c. network analyser had already been built at the University, and it would be of assistance if this apparatus could be used in the final computer.

It was therefore decided to replace the machine units in the network analyser by d.c. analogue simulators, so that steady state investigations could be carried out as before, but transient studies done in addition.

In this investigation a simple representation of a generator, where only the mechanical equation of motion is solved, was chosen to start with. Provision was made so that the effects of a governor, voltage regulator and damping could be added.

By using a new method of controlling the phase angle of an oscillator feeding an a.c. network analyser, it is possible for the simulator to run asynchronously. One of the shortcomings of all methods of simulation (except micro-machines) is that they do not allow prolonged asynchronous running of the generator model.^{26.} Once the governor and voltage regulator analogues have been added to the existing apparatus, it is hoped that pole slipping and resynchronisation, and asynchronous operation can be simulated without further modification.

2. PROPERTIES OF AN ALTERNATOR

2.1. Internal emf. and reactance

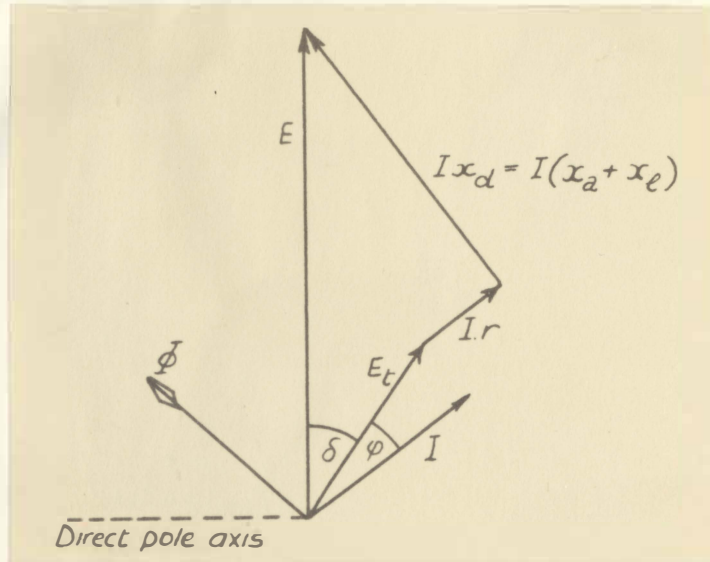


Fig.2.1. Simplified vector diagram of a cylindrical-rotor machine.

Figure 2.1. is the simplified vector diagram of a cylindrical-rotor generator on load. The field current produces a flux in the direct axis of the machine, which induces an emf. E , lagging 90° behind the flux. Due to the load current I flowing in the machine, an armature reaction flux is produced. Furthermore, I causes a leakage flux to exist, in the air gap. These fluxes add to the no-load flux resulting in flux Φ in the machine. Φ induces an emf. which is the terminal emf. E_t of the machine, plus the $I r$ drop due to the armature resistance. 27.

The difference between E and E_t can be regarded as a voltage drop due to the load current flowing through an armature reaction reactance x_a ,

a leakage.....

a leakage reactance x_l and the armature resistance r . The synchronous reactance x_d is the sum of x_a and x_l .

The above applies when the generator is working under steady-state conditions. During transient disturbances, the above values of internal emf. and synchronous reactance no longer apply as such, and the vector diagram must be modified, as is shown in figure 2.2, where the transient vectors have been superimposed on the steady-state vectors.

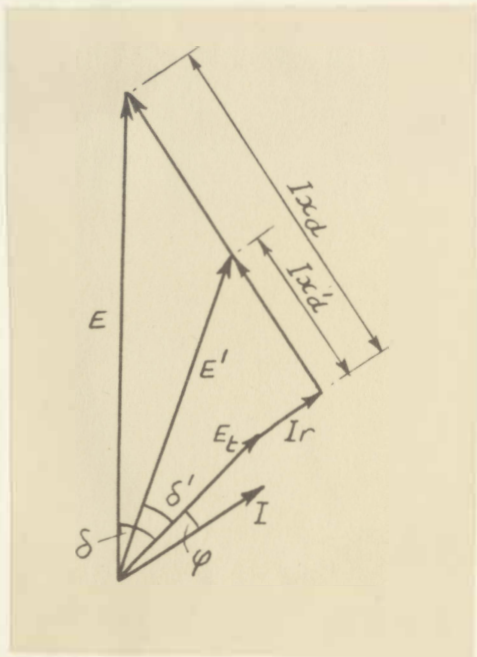


Fig.2.2. Simplified vector diagram of a cylindrical-rotor generator for transient conditions.

Instead of E , x_d and δ the corresponding transient quantities E' , x_d' and δ' are used. E' is a fictitious emf. which would cause load current I to flow through the transient reactance x_d' of the generator.

When.....

When the generator is a salient pole machine instead of a cylindrical-rotor machine, the armature reaction flux produced by the armature current does not affect the flux produced by the field current so much. Apart from this the above description applies to a salient-pole machine.

From the vector diagrams in figures 2.1. and 2.2 we see that the generator can be represented by a zero impedance generator behind an impedance. The emf. will be the internal emf. E of the machine and the impedance will consist of the armature resistance r and the leakage and armature reaction reactances. During steady-state running the appropriate steady-state values are to be used, and transient values under transient conditions.

The electrical power output of the generator, including $I^2 r$ losses, is given by:

$$P_e = 3.E.I.\cos(\delta+\phi) \quad (\text{see figure 2.1})$$

where E = line to neutral rms. voltage.

I = line to neutral rms. current.

2.2. Inertia and stored energy.

When a generator is running under steady-state conditions, its electrical output is equal to the mechanical input from the prime mover (i.e. when losses are neglected). If either of these quantities were to change suddenly, the rotor of the machine would speed up or slow down,

depending.....

depending on whether the input were more or less than the output. This change in the relative position of the rotor is seen as a change in the internal angle δ of the machine.

Because of the large inertia of the rotating masses of the generator and prime mover, the rotor cannot change its position instantaneously following a disturbance. This has an important effect on the transient behaviour of a generator, and on its stability after a disturbance.

The inertia of a generator is usually given in terms of an "inertia constant" H , which is proportional to the kinetic energy of the moving parts of the machine by virtue of their movement.²⁸

H is given by:

$$H = \frac{0.231 \cdot 10^{-6} \cdot I \cdot v^2}{P} \quad \text{KW sec/KVA}$$

where I = moment of inertia of rotor of generator and prime mover, lb.-ft.².

v = speed, r.p.m.

P = Power rating of the machine, KVA.

2.3. Dynamic equation of the machine.

When a generator runs in synchronism with a power system to which it is connected, the equation of equilibrium which must be satisfied is, in terms of power:

$$P_{\text{input}} = P_{\text{inertia}} + P_{\text{damping}} + P_{\text{output}} \quad (2.3-1)$$

(because the machine's speed does not differ much from synchronous speed

during.....

during transient conditions, equation 2.3-1 can be written in terms of power, and not torque).

Substituting values in the respective components of equation 2.3-1 gives the general differential equation for a synchronous generator connected to a power system:

$$P_{\text{input}} = M \frac{d^2\delta}{dt^2} + K_d \frac{d\delta}{dt} + 3.E.I.\cos(\delta+\phi) \quad (2.3-2)$$

where P_{input} = mechanical power input less mechanical losses, KW

$$M = \frac{P.H_0}{\pi.f}$$

= inertia constant, KW sec/el.rad. per sec.

P = rated power of the machine, KVA

f = rated frequency, c/s

δ = angular displacement between the internal emf. of the machine and the infinite busbar voltage, radians.

K_d = damping coefficient, KW/el.rad. per sec. (see appendix A)

E = internal emf. of machine, KV. rms. line to neutral

I = load current, A. rms. line to neutral

ϕ = phase angle between I and the voltage of the infinite busbar, radians.

3. The.....

3. THE SIMULATION OF A SYNCHRONOUS GENERATOR

3.1. Derivation of the analogue representation

The simulator to be described was intended to be a simple representation of a machine to start with, with provision for adding simulation of secondary effects, such as voltage regulator action, governor response and damping.

The following simplifying assumptions were made: ²⁹

1. Transient saliency neglected.
2. Flux linkages held constant, corresponding to the voltage behind the transient reactance.
3. Damping torque and subtransient effects neglected.
4. Constant mechanical input power to the machine.
5. Saturation effects neglected.

Taking these assumptions into account, the simulator must satisfy the following equation:

$$P_{\text{input}} = M \frac{d^2\delta}{dt^2} + 3.E.I.\cos(\delta+\phi) \quad (3.1-1)$$

(the symbols are the same as in equation 2.3-2)

where P_{input} , M and E are constant quantities for a particular problem.

Rewriting equation 3.1-1:

$$M \frac{d^2\delta}{dt^2} = P_{\text{input}} - 3.E.I.\cos(\delta+\phi)$$

Integrating.....

Integrating, and dividing by M:

$$\frac{d\delta}{dt} = \frac{1}{M} \int \left[P_{\text{input}} - 3.E.I.\cos(\delta+\phi) \right] dt \quad (3.1-2)$$

As will be shown in the following pages, the simulator circuit has a closed loop transfer function which is similar to equation 3.1-2.

A block diagram of the generator simulator in its simplest form is shown in figure 3.1 The device consists of a variable frequency oscillator which feeds the a.c. network analyser through a power amplifier with a very low output impedance, and an impedance. The amplifier output voltage represents the internal emf. of the generator, and the impedance the internal impedance of the machine.

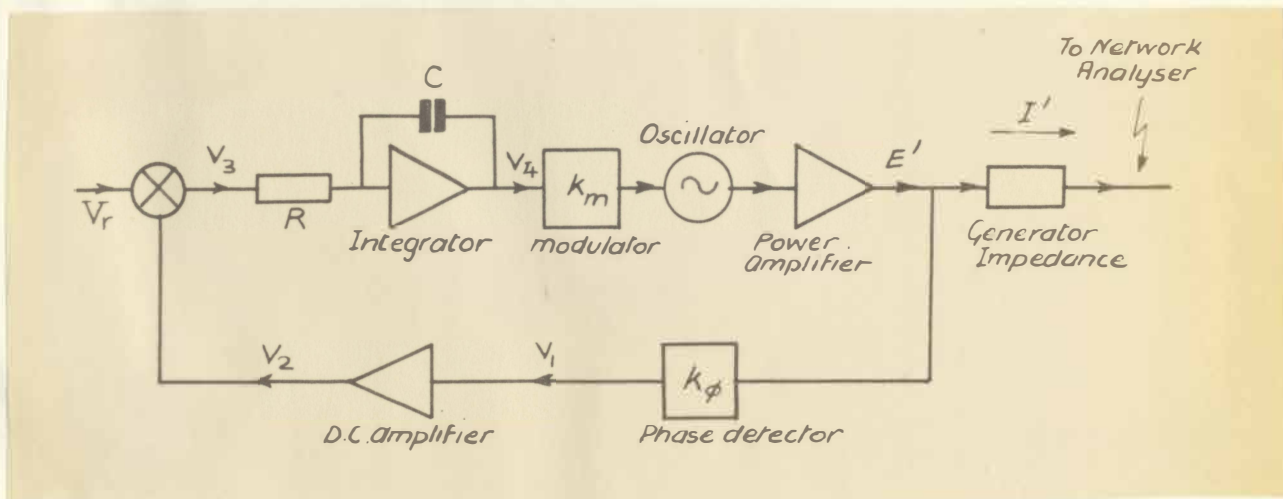


Fig. 3.1 Block diagram of the generator simulator.

The power output of the power amplifier is given by:

$$P_{\text{output}} = E' I' \cos (\delta + \phi) \quad (3.1-3)$$

where E' = power amplifier output voltage

I' = output current of the amplifier

$(\delta + \phi)$ = phase angle between E' and I'

The phase detector output is a d.c. voltage proportional to the in-phase component of the load current of the power amplifier (see appendix B).

Referring to figure 3.1 and equation 3.1-3.

$$v_1 = k_{\phi} I' \cos(\delta + \phi) \quad (3.1-4)$$

where k_{ϕ} = the transfer constant of the phase detector.

Providing E' remains constant, the phase detector output therefore is a measure of the power output of the power amplifier.

The phase detector output is fed to a d.c. amplifier, whose output is given by:

$$\begin{aligned} v_2 &= A_{\text{dc}} \cdot k_{\phi} I' \cos (\delta + \phi) \\ &= k I' \cos (\delta + \phi) \end{aligned} \quad (3.1-5)$$

where $k = A_{\text{dc}} \cdot k_{\phi}$

The d.c. amplifier output v_2 is taken to a summing point, where it is subtracted from a d.c. voltage V_r . The resultant voltage is given by:

$$\begin{aligned} v_3 &= V_r - v_2 \\ &= V_r - k I' \cos (\delta + \phi) \end{aligned} \quad (3.1-6)$$

The.....

The integrator output is:

$$v_4 = \frac{1}{RC} \int \left[V_r - k I' \cos (\delta + \phi) \right] dt \quad (3.1-7)$$

This voltage is applied to the modulator which controls the oscillator frequency. The oscillator frequency and the modulator input are related by the modulator transfer constant k_m , viz:

$$\begin{aligned} k_m &= \frac{\text{oscillator frequency change}}{\text{modulator input voltage}} \text{ rad. per sec/volt.} \\ &= \frac{\Delta \omega}{v_4} \end{aligned} \quad (3.1-8)$$

Substituting equation 3.1-8 in equation 3.1-7:

$$\Delta \omega = \frac{k_m}{RC} \int \left[V_r - k I' \cos (\delta + \phi) \right] dt \quad (3.1-9)$$

The oscillator frequency corresponds to the base frequency of the network analyser when the input to the modulator is zero. Applying a signal to the modulator will increase or decrease the oscillator frequency, depending upon the polarity of the applied voltage,

Thus the instantaneous oscillator frequency is given by:

$$\omega = \omega_0 \pm \Delta \omega \quad (3.1-10)$$

where ω_0 = oscillator frequency with no modulating voltage

= network analyser base frequency

$\Delta \omega$ = change in ω_0 due to the application of a modulating signal.

If δ is the angular displacement between E' , the power amplifier output voltage, and the network analyser system voltage, the instantaneous

difference.....

difference frequency $\Delta \omega$ between ω_0 , the network analyser base frequency and ω , the instantaneous frequency of the oscillator can be expressed as:

$$\Delta \omega = \frac{d\delta}{dt} \quad (3.1-11)$$

Equation 3.1-8 can be re-written as:

$$\frac{d\delta}{dt} = \frac{k_m}{RC} \int \left[V_r - k I' \cos(\delta + \phi) \right] dt \quad (3.1-12)$$

This expression can be seen to be very similar to equation 3.1-2, and the analogy is based on this.

The circuit works as follows: When the power amplifier feeds some current into the network analyser, to which some other oscillator representing infinite busbars, say, is connected, the two power sources are adjusted to run in synchronism. The phase detector gives some output voltage, which, after it is amplified, is cancelled by an equal and opposite reference voltage V_r . The integrator now receives no signal, with the result that its output is zero. With no input signal to the modulator, the oscillator runs at the base frequency of the network analyser.

If some disturbance now occurs, say a change in the impedance between the generator simulator and the other oscillator, the phase detector output changes. The integrator input is now no longer zero, since the amplified output of the phase detector no longer balances the reference voltage. The integrator output now changes at a rate determined by the time constant of the integrator, and the amplitude of the unbalance voltage, and the oscillator frequency changes correspondingly.

As soon....

As soon as the instantaneous frequency changes, the phase angle between the two oscillator voltages also changes. The phase detector senses the change in phase angle and the corresponding change in load current, and its output changes once more in such a sense so as to oppose the change in frequency.

The simulator thus is a closed loop negative feedback control circuit. During steady state operation the phase angle with which the simulator runs, is determined by the reference voltage. Provided the angle is not greater than 90° , the simulator will run in stable synchronism with the other sources in the network analyser.

If a disturbance occurs, such as a change of load or the occurrence and clearing of a fault, the frequency of the simulator oscillator changes, but its rate of change is controlled by the integrator time constant. The rate of change of phase angle is thus controlled by the integrator, and the amplitude of the change in the phase angle by the output of the phase detector. Following a disturbance the phase angle therefore varies periodically, until it eventually settles down to a new steady state value. If, however, the disturbance lasts too long or is too big the phase angle will increase beyond a critical value, determined by the integrator time constant and the magnitude of the reference voltage, and the simulator will lose synchronism with the rest of the system.

3.2. Scaling of the analogue simulator

To distinguish between actual machine quantities and analogue quantities, primed letters will be used to denote that they refer to the analogue. Unprimed letters refer to the actual generator. Since the scale factor relating phase angles in the simulator and in the real machine is unity, unprimed letters representing phase angles will be used in both cases.

Referring to equation 3.1-2 page 10, the equation describing the performance of a generator is:

$$\frac{d\delta}{dt} = \frac{1}{M} \int \left[P_{\text{input}} - 3.E.I. \cos(\delta+\phi) \right] dt \quad (3.2-1)$$

making $\Delta P = P_{\text{input}} - 3.E.I. \cos(\delta+\phi)$ gives: (3.2-2)

$$\frac{d\delta}{dt} = \frac{1}{M} \int \Delta P. dt \quad (3.2-3)$$

Equation 3.1-12 (page 13) can be written as:

$$\frac{d\delta}{dt'} = \frac{k_m}{RC} \int \left[V_r - k.I'.\cos(\delta+\phi) \right] dt \quad (3.2-4)$$

putting $\Delta V = V_r - k.I'.\cos(\delta+\phi)$ gives; (3.2-5)

$$\frac{d\delta}{dt'} = \frac{k_m}{RC} \int \Delta V. dt. \quad (3.2-6)$$

The network analyser base frequency is 500 c/s. To keep a one to one ratio between frequency and time, the time scale of the simulator has to be reduced by the same factor that the analyser frequency is higher than the machine frequency.

Let.....

Let $\alpha = \frac{\text{machine frequency}}{\text{analyser frequency}}$

$$\alpha = \frac{\text{analyser time}}{\text{real time}}$$

$$= \frac{t'}{t} \text{ sec/sec.}$$

i.e. $t' = \alpha.t.$

i.e. $dt' = \alpha.dt$ (3.2-7)

Let $\beta = \frac{\text{d.c. analogue "power"}}{\text{machine power}}$

$$= \frac{\Delta V}{\Delta P} \text{ volts/watt} \quad (3.2-8)$$

Substitute equations 3.2-7 and 3.2-8 in equation 3.2-6

$$\frac{d\delta}{\alpha \cdot dt} = \frac{k_m}{RC} \int (\beta \cdot \Delta P) \alpha \cdot dt$$

i.e. $\frac{d\delta}{dt} = \alpha^2 \cdot \beta \cdot \frac{k_m}{RC} \int \Delta P \cdot dt$ (3.2-9)

Compare this with equation 3.2-3. The two are identical provided:

$$\frac{1}{M} = \frac{\alpha^2 \cdot \beta \cdot k_m}{RC} \quad (3.2-10)$$

Equation 3.2-10 gives the relation between the inertia constant M of a generator, and the constants of the d.c. analogue circuit.

Referring back, substitute equation 3.2-8 in equation 3.2-5:

$$\begin{aligned} \Delta P &= \frac{1}{\beta} \left[V_r - k \cdot I' \cdot \cos(\delta + \phi) \right] \\ &= \frac{V_r}{\beta} - \frac{k}{\beta} \cdot I' \cos(\delta + \phi) \end{aligned} \quad (3.2-11)$$

The.....

The first term in the right hand side corresponds with P_{input} in equation 3.2-2.

$$\begin{aligned} \text{Let } \gamma &= \frac{\text{a.c. analyser base power}}{\text{system base power}} \\ &= \frac{P'}{P} \quad VA/VA \end{aligned} \quad (3.2-12)$$

$$\begin{aligned} \text{Let } \epsilon &= \frac{\text{a.c. analyser base voltage}}{\text{system base voltage}} \\ \text{i.e. } \epsilon &= \frac{E'_r}{E_r} \quad \text{volt/volt} \end{aligned} \quad (3.2-13)$$

$$\begin{aligned} \text{Now } I' &= \frac{P'}{E'_r} \\ \text{and } I &= \frac{P}{3E_r} \end{aligned} \quad (3.2-14)$$

$$\text{i.e. } \frac{P}{E_r} = 3I \quad (3.2-15)$$

Substituting equations 3.2-12 and 3.2-13 in equation 3.2-14 gives:

$$\begin{aligned} I' &= \frac{\gamma \cdot P}{\epsilon \cdot E_r} \\ \text{i.e. } \frac{P}{E_r} &= \frac{\epsilon}{\gamma} \cdot I' \end{aligned}$$

Equating this with equation 3.2-15 gives the relation between I and I' , viz:

$$I' = \frac{\gamma}{\epsilon} \cdot 3I \quad (3.2-16)$$

Substituting equation 3.2-15 in the second term of equation 3.2-11 gives:

$$\Delta P = \frac{V_r}{\beta} - \left[\frac{k}{\beta} \cdot \frac{\gamma}{\epsilon} \cdot 3 \cdot I \cdot \cos(\delta + \phi) \right]$$

The.....

The second term on the right hand side is similar to that in equation 3.2-2. Equating them gives:

$$\frac{k \cdot \gamma}{\beta \cdot \varepsilon} = E \quad (3.2-17)$$

From equation 3.2-10 we have:

$$RC = \alpha^2 \cdot \beta \cdot k_m \cdot M.$$

Substituting equation 3.2-17 and the expression for M given in equation 2.3-2, in the above equation, gives:

$$RC = \alpha^2 \cdot \frac{k \cdot \gamma}{\varepsilon \cdot E} \cdot k_m \cdot \frac{H \cdot P}{\pi \cdot f}$$

$$\text{but } \gamma = \frac{P'}{P} \quad (\text{from equation 3.2-12})$$

$$\text{and } \varepsilon = \frac{E'_r}{E_r} \quad (\text{from equation 3.2-13})$$

$$\text{hence } RC = \alpha^2 \cdot k \cdot \frac{P'/P}{(E'_r/E_r)E} \cdot k_m \cdot \frac{H \cdot P}{\pi \cdot f}$$

Simplifying, and noting that E/E_r is the per-unit value of the generator internal emf., gives:

$$RC = \frac{\alpha^2 \cdot k \cdot k_m \cdot p' \cdot H}{\pi \cdot E'_r \cdot f \cdot E_{p.u.}} \quad (3.2-18)$$

$$\text{where } E_{p.u.} = E/E_r$$

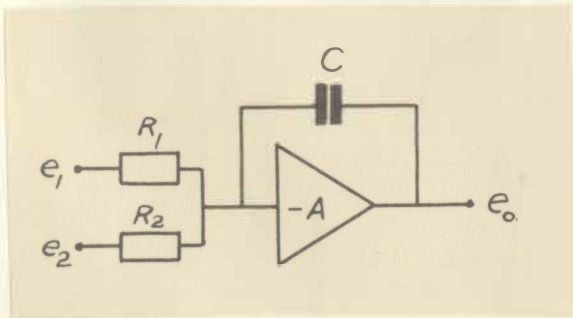
By substituting the relevant figures in equation 3.2-18, the generator simulator constants for a particular problem can be calculated.

3.3. Derivation of the Analogue with damping included

The intention was to build a basic generator simulator, to which a damping circuit could afterwards be added. It was found, however, that stable operation of the simulator, when synchronised with "infinite busbars" could not be obtained unless damping was added. Of necessity a damping circuit and its analyses had to be included.

Sections 3.1 and 3.2 give the derivation of the generator simulator equation and how the simulator is scaled, but neglecting the damping term that appears in the machine swing equation (see equation 2.3-2 page 8). The circuit, shown in block diagram form in figure 3.1 (page 10) must be modified to include the effect of damping. More specifically, the integrator must be changed, by adding a feedback loop to it.

Figure 3.2 shows the diagram of an ordinary summing integrator,³² as is used in the generator simulator. Figure 3.3 shows how this circuit is extended to include damping.



$$- e_o = \frac{1}{R_1 C_1} \int e_1 . dt + \frac{1}{R_2 C_2} \int e_2 . dt$$

Fig. 3.2_ Summing integrator block diagram.

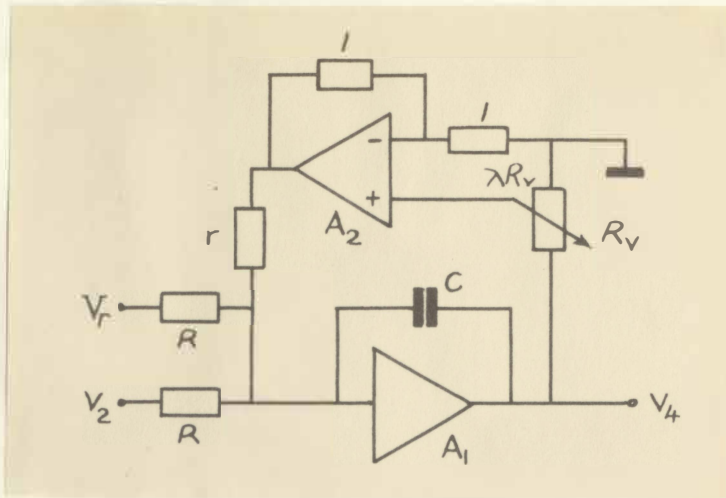


Fig.3.3 Block diagram of the integrator with a damping loop.

The circuit shown in fig.3.3 was used in place of the integrator shown in fig.3.1 (page 10). Voltages V_r , v_2 and v_4 are the same as those in fig.3.1 and in the ensuing derivation of the analogue loop equation.

We now have:

$$v_4 = \frac{1}{RC} \int \left[V_r + v_2 - \frac{2 \cdot \lambda \cdot R}{r} \cdot v_4 \right] dt. \quad (\text{see appendix C}) \quad (3.3-1)$$

where $v_4 = \frac{d\delta}{dt} / k_m$

and $v_2 = -k \cdot I' \cdot \cos(\delta + \phi)$

Substituting these expressions for v_2 and v_4 in the above equation we get:

$$\frac{d\delta}{dt} = \frac{k_m}{RC} \int \left[V_r - k \cdot I' \cdot \cos(\delta + \phi) - \frac{2 \cdot \lambda \cdot R}{k_m \cdot r} \cdot \frac{d\delta}{dt} \right] dt \quad (3.3-2)$$

This.....

This expression is seen to be similar to the generator swing equation with the damping term included, viz:

$$\frac{d\delta}{dt} = \frac{1}{M} \int \left[P_{\text{input}} - 3.E.I.\cos(\delta+\phi) - K_d \cdot \frac{d\delta}{dt} \right] dt$$

The coefficient $\frac{2.\lambda.R}{k_m.r}$ in the third term of equation 3.3-2 corresponds to the damping coefficient K_d in the above expression.

3.4. Scaling the generator simulator, including damping effects

Repeating the procedure of section 3.2, equation 3.3-2 finally appears as:

$$\frac{d\delta}{dt} = \frac{\alpha^2 \cdot k_m}{RC} \int \Delta V \cdot dt$$

where $\Delta V = V_r - k.I' \cos(\delta+\phi) - \frac{2.\lambda.R}{\alpha.k_m.r} \cdot \frac{d\delta}{dt}$

now $\Delta P = P_{\text{input}} - 3.E.I.\cos(\delta+\phi) - K_d \cdot \frac{d\delta}{dt}$

putting $\Delta V = \beta.\Delta P$, and substituting this in the expression for ΔV , we get:

$$\Delta P = \frac{1}{\beta} \left[V_r - k.I' \cos(\delta+\phi) - \frac{2.\lambda.R}{\alpha.k_m.r} \cdot \frac{d\delta}{dt} \right]$$

$\frac{2.\lambda.R}{\beta.\alpha.k_m.r}$ corresponds to K_d in the former expression for ΔP ,

i.e. the analogue damping constant K_d^1 is given by:

$$K_d^1 = \frac{2.\lambda.R}{\alpha.k_m.r.\beta} \quad (3.3-3)$$

From.....

From equation 3.2-17 we have:

$$\beta = \frac{k \cdot \gamma}{\epsilon \cdot E}$$

but $\gamma = P' / P$ (from equation 3.2-12)

and $\epsilon = E'_r / E_r$ (from equation 3.2-13)

thus $\beta = \frac{k \cdot (P' / P)}{(E'_r / E_r) E}$

$$= \frac{k \cdot P'}{E'_r \cdot E_{p.u.} \cdot P}$$

where $E_{p.u.} = E'_r / E_r$

Substituting this expression for β in equation 3.3-3 gives :

$$K'_d = \frac{2 \cdot \lambda \cdot R}{\alpha \cdot k_m \cdot r} \cdot \frac{E'_r \cdot E_{p.u.} \cdot P}{k \cdot P'} \quad (3.3-4)$$

Using equation 3.3-4 the damping coefficient of the generator simulator can be calculated.

4. EXPERIMENTAL RESULTS

To check the accuracy of the simulator, a comparison between measured and calculated results for a single machine connected to infinite busbars was made. Three tests are required,²⁵ i.e. (i) a steady-state power-angle curve, (ii) a transient-stability study and (iii) a transient test on the integrator.

4.1. Steady-state test

The circuit used to measure the variation of "electrical power" as a function of the internal angle δ is shown in fig.4.1a.

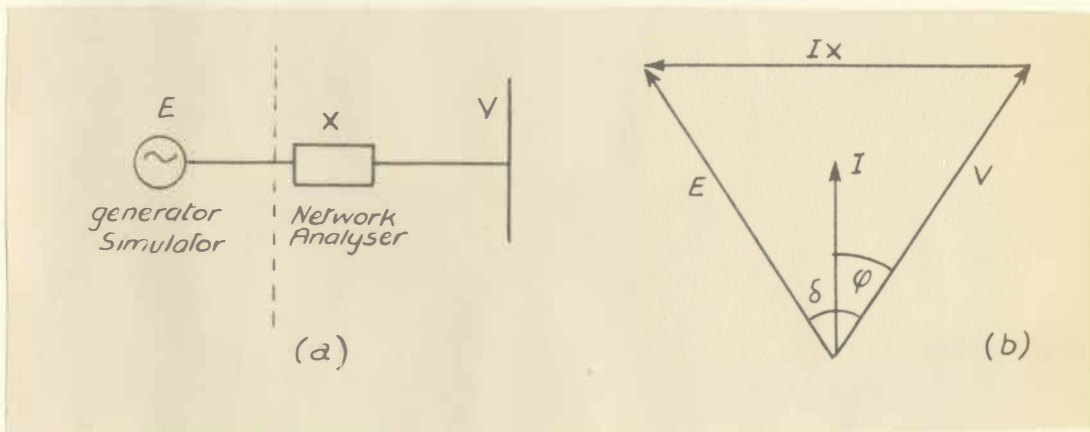


fig.4.1. Diagram of circuit used for steady-state test and the corresponding vector diagram.

In fig. 4.1b. the vector diagram showing the relation of the voltages in the circuit is given.

The current flowing between the generator simulator and the infinite busbar model is given by:

$$I = \frac{1}{X} \sqrt{E^2 + V^2 - 2.E.V.\cos \delta} \quad (4.1-1)$$

The.....

The electrical power, appearing as a d.c. voltage in the generator analogue, is:

$$P_e = k.I.\cos(\delta + \phi) \quad (\text{see appendix E})$$

When $E = V, -\phi = \frac{\delta}{2}$, as shown in fig. 4.1b. The expression for P_e now reduces to

$$P_e = k.I.\cos \frac{\delta}{2} \quad (4.1-2)$$

Substituting figures in equations 4.1-1 and 4.1-2, values of P_e can be calculated. Fig.4.2 shows the calculated curve of P_e vs. δ , and measured results.

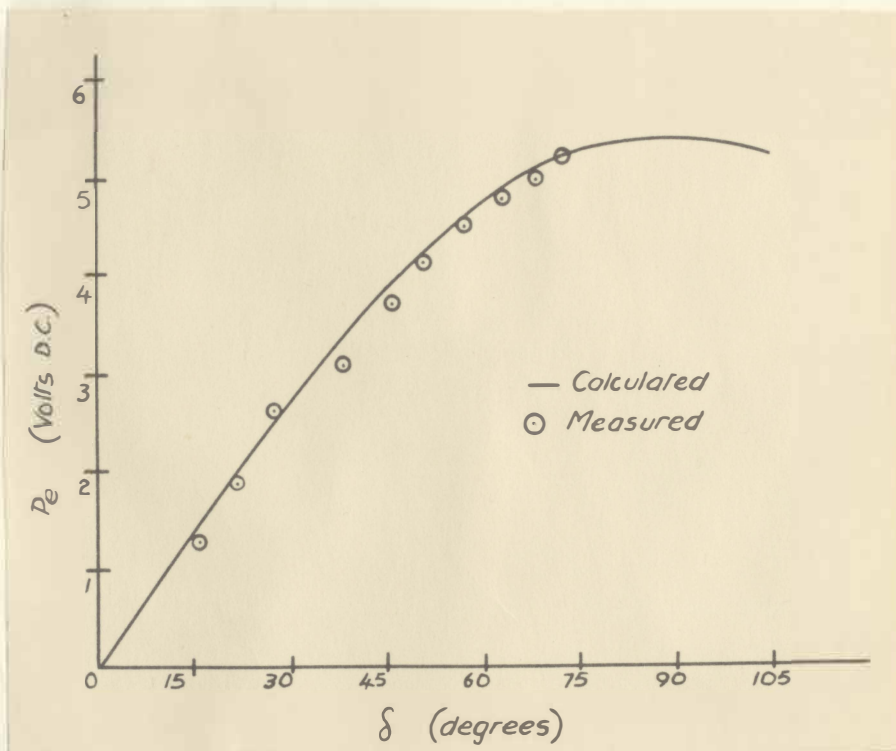


fig.4.2 Steady-state power angle curve.

$f = 500$ c/s

$E = V = 10$ V r.m.s.

$X = 2.1$ K.ohm

$k = 1.143$ V_{d.c.} / m.A._{rms.}

P_e was.....

P_e was measured at the output terminals of the d.c. amplifier in the feed-back loop of the simulator circuit (see fig. 3.1, p. 10). The internal angle δ was measured by a phase angle recorder,³³. (see appendix F)

4.2. Transient stability study

Two transient stability problems were simulated with the generator model. It was found that with zero damping the simulator was unstable when connected to infinite busbars through an impedance. A damping circuit, as described in section 3.3 p.19 was added to the analogue circuit to allow synchronous operation of the simulator and the infinite busbar generator of the network analyser.

4.2.1. Transient stability. Study 1

The details of the problem are given in ref. 34. Fig. 4.3 shows the system interconnection:

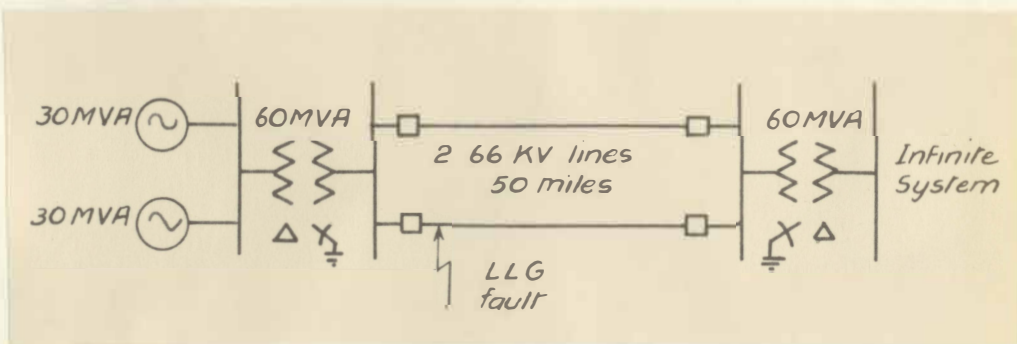


fig.4.3 Diagram of system being studied.

A zero-impedance double-line-to-ground fault occurs at the sending end of one of the transmission lines. The faulted line is then disconnected at both ends to isolate the fault. Providing the fault is cleared fast enough, the sending-end machines remain in synchronism with the infinite system.

The....

The sending-end generators can be represented by one equivalent generator. During transient conditions this generator behaves like a zero-impedance voltage source behind the transient reactance of the generator (see page 9, where the qualifying assumptions for the above representation are listed).

Scaling of the generator simulator can be done by substituting the appropriate values in equation 3.2-18 (page 18). This equation is:

$$RC = \frac{\alpha^2 \cdot k \cdot k_m \cdot P^t}{\pi \cdot E_r^t \cdot f} \cdot \frac{H}{E_{p.u.}}$$

The following machine constants are given in ref.35:

- E = 42.9 KV line to neutral
= Generator transient internal emf.
- V = 38.1 KV line to neutral
= Base voltage of the system
- H = 3 KW sec/KVA
= Inertia constant
- f = 60 c/s
= Rated frequency

The generator simulator constants (see section 3.2) are as follows:

- k = 0.254 V/mA (see appendix E)
- k_m = 12.2 rad.per.sec/V
- f^t = 500 c/s
= network analyser base frequency

$$P^{\#} = 100 \text{ mW}$$

= network analyser base power

$$E_r^{\#} = 10\text{V}$$

= network analyser base voltage

$$E_{\text{p.u.}} = \frac{42.9 \text{ KV}}{38.1 \text{ KV}}$$

= 1.125 p.u.

$$a = \frac{60 \text{ c/s}}{500 \text{ c/s}}$$

= 0.12

Substitution in the expression for RC gives:

$$RC = 6.31 \text{ m. sec.}$$

A convenient value for R is 120 K.ohm. Using this value of resistance gives:

$$C = 0.0527 \mu\text{F.}$$

C and R are set to the values given above. They represent the inertia of the generator.

The swing curves shown in ref.34 were calculated, assuming zero damping. As explained in section 3.3 it was necessary to have some damping in the simulator circuit. Provided the minimum damping required in the simulator is less than the damping of the machines to be simulated, the damping of the simulator can always be set to a figure corresponding to the damping of the generator.

For.....

For this study the simulator was run with minimum damping, which was the closest possible approach to the calculated case, where zero damping was assumed. It is shown in appendix D that the damping coefficient of a typical generator of this type is more than the damping coefficient of the generator simulator.

The a.c. network analyser was set up according to the figures given in ref. 34. They are:

$$E' = 1.125 \text{ p.u.}$$

= generator simulator output voltage

$$V' = 0.95 \text{ p.u.}$$

= infinite system voltage

$$X_1 = 0.679 \text{ p.u.}$$

= tie reactance before the fault occurs

$$X_2 = 2.9 \text{ p.u.}$$

= tie impedance during the fault

$$X_3 = 0.961$$

= impedance after the fault has been cleared.

Network analyser base voltage = 10V

Network analyser base impedance = 1000 ohms.

The tie impedances were switched with a high speed relay circuit (see appendix F) so that the fault clearing time could be changed. By adjusting the reference voltage in the generator simulator circuit the initial internal angle was set to the value calculated in ref. 34. The

reference.....

reference voltage control could be calibrated in terms of power, and by setting the reference voltage to its calculated value, the initial angle would automatically be right. However, the calibration would have to be changed for every problem set up on the simulator. Therefore the former method was used. The variation of internal angle after the start of the fault was measured by the apparatus described in ref. 33 (see also appendix F) and its output was displayed on a storage tube oscilloscope.

The resultant swing curves, for three fault clearing times, are shown in fig.4.4 together with calculated curves from reference 34.

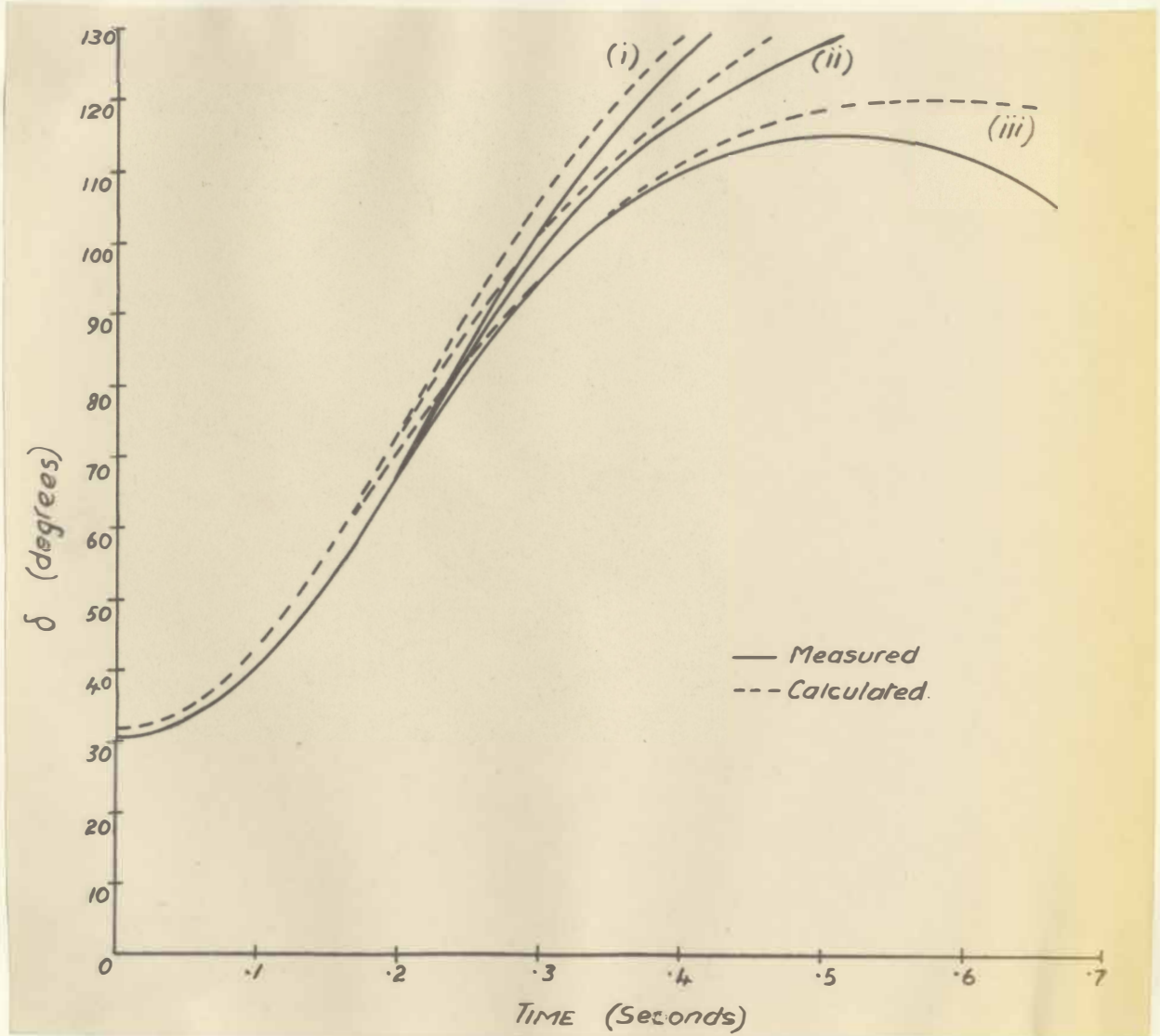


fig.4.4. Measured and calculated swing curves.
(i) fault cleared in 0.17 sec.
(ii) fault cleared in 0.16 sec.
(iii) fault cleared in 0.15 sec.

4.2.2. Transient stability. Study 2

This problem was taken from ref. 28 (pp.44-49). The system consists of a generator delivering power through two parallel transmission lines to a large system as shown in fig.4.5. A three-phase short occurs in the middle of one of the lines, and is cleared by the simultaneous disconnection of the two ends of that line.

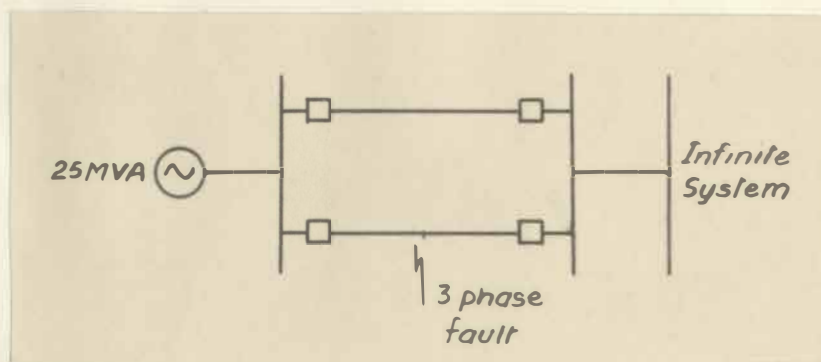


fig. 4.5. Diagram of the system.

The settings of the simulator's integrator constants can be calculated, as in the previous example, by substituting the figures given in the following equation:

$$RC = \frac{\alpha^2 \cdot k \cdot k_m \cdot P^t}{\pi \cdot E_r' \cdot f} \cdot \frac{H}{E_{p.u.}}$$

Given: $E_{p.u.} = 1.03$ p.u.

= voltage behind the transient reactance of the generator.

$H = 2.76$ KW sec/KVA

= inertia constant of the generator

$f = 60$ c/s

= rated frequency of the system.

The simulator constants are the same as in section 4.2.1.

Substitution in the expression for RC gives:

$$RC = 6.34 \text{ m.sec.}$$

Again taking R as 120 K.ohms, gives:

$$C = 0.0529 \mu\text{F.}$$

The swing curves, shown in fig. 4.6 were taken with the damping of the circuit set to the minimum value allowing stable steady-state operation. Although figures are not given in the problem, since zero damping was assumed, typical figures for a generator of this type give a damping coefficient $K_d = 5.2 \cdot 10^{-4}$ KW.sec/KVA degree. The simulator damping corresponds to a damping coefficient $K'_d = 7.6 \cdot 10^{-4}$ KW.sec/KVA degree (see appendix D).

The damping coefficient of the simulator is $1\frac{1}{2}$ times higher than the typical figure for a 25 MVA waterwheel generator. In appendix D a reason for this is given, and a suggestion made how to reduce the damping coefficient of the simulator to a more acceptable value.

Using a base of 10V and 1000 ohms, the following quantities were set on the a.c. network analyser:

$$E' = 1.03 \text{ p.u.}$$

= generator simulator output voltage

$$V' = 1.00 \text{ p.u.}$$

= infinite busbar voltage

$$X_1 = 0.40 \text{ p.u.}$$

= pre-fault tie reactance

$$X_2 = 1.10 \text{ p.u.}$$

= tie reactance for the duration of the fault.

X_3

$$X_3 = 0.50 \text{ p.u.}$$

= post-fault tie reactance.

Swing curves were recorded for various fault clearing times, as shown in fig.4.6.

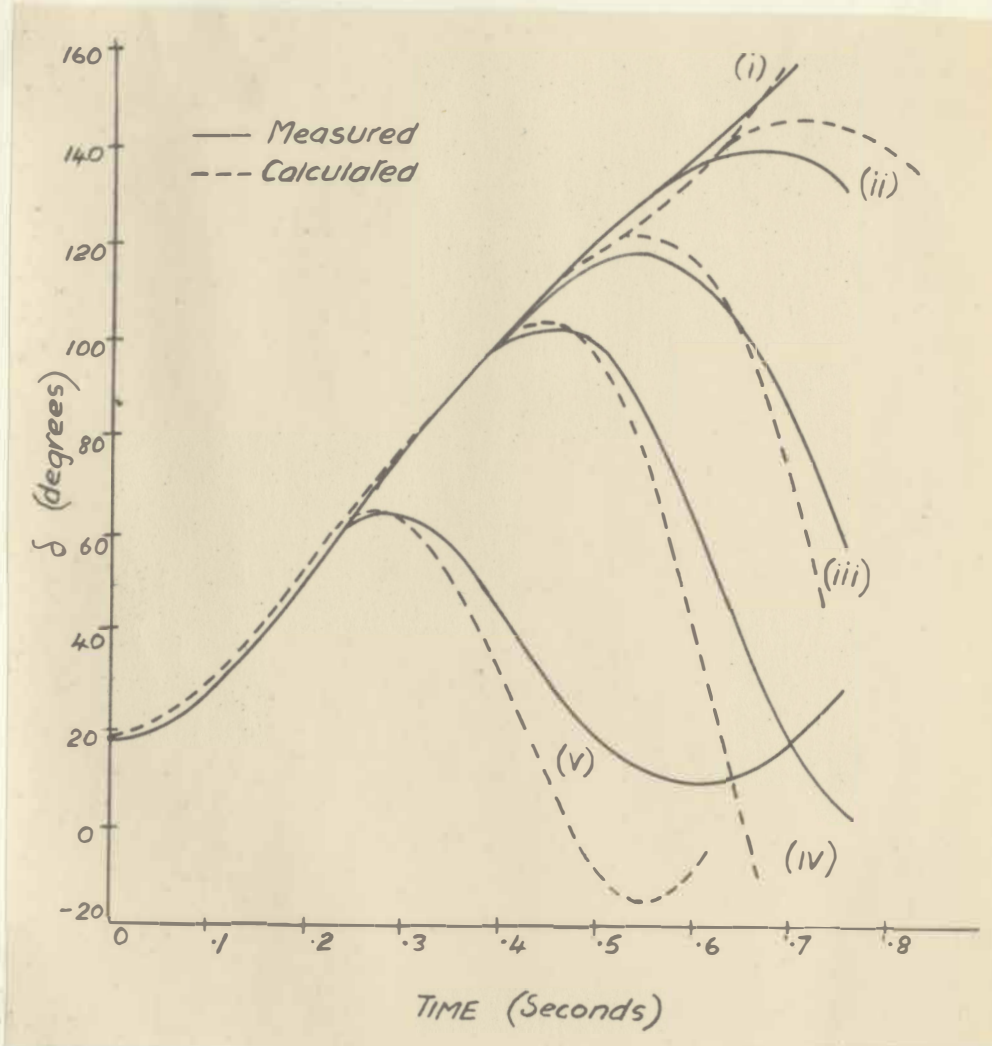


fig. 4.6. Swing curves - Study 2.

- (i) sustained fault
- (ii) fault cleared in 0.6 sec.
- (iii) fault cleared in 0.5 sec.
- (iv) fault cleared in 0.4 sec.
- (v) fault cleared in 0.2 sec.

4.3. Integrator transient test

The integrator in the d.c. analogue section of the generator simulator was checked for accuracy by applying a step voltage to the integrator input, and observing how the output voltage changed with respect to time.

For a step input, the output voltage of an ideal integrator, as given by ref.32 is:

$$-e_{out} = e_{in} \frac{t}{RC} \quad (4.3-1)$$

where e_{out} = integrator output voltage

e_{in} = integrator input voltage

R = integrator input resistor

C = integrator feedback capacitor

t = time.

In this test a step of -40 mV. was applied to the integrator input. Substituting the following figures in equation 4.3-1 gives the results which are plotted in fig.4.7, together with the measured curve.

$$e_{in} = - 40 \text{ mV}$$

$$R = 120 \text{ K.ohm}$$

$$C = 0.256 \text{ } \mu\text{F}$$

fig.4.7.....

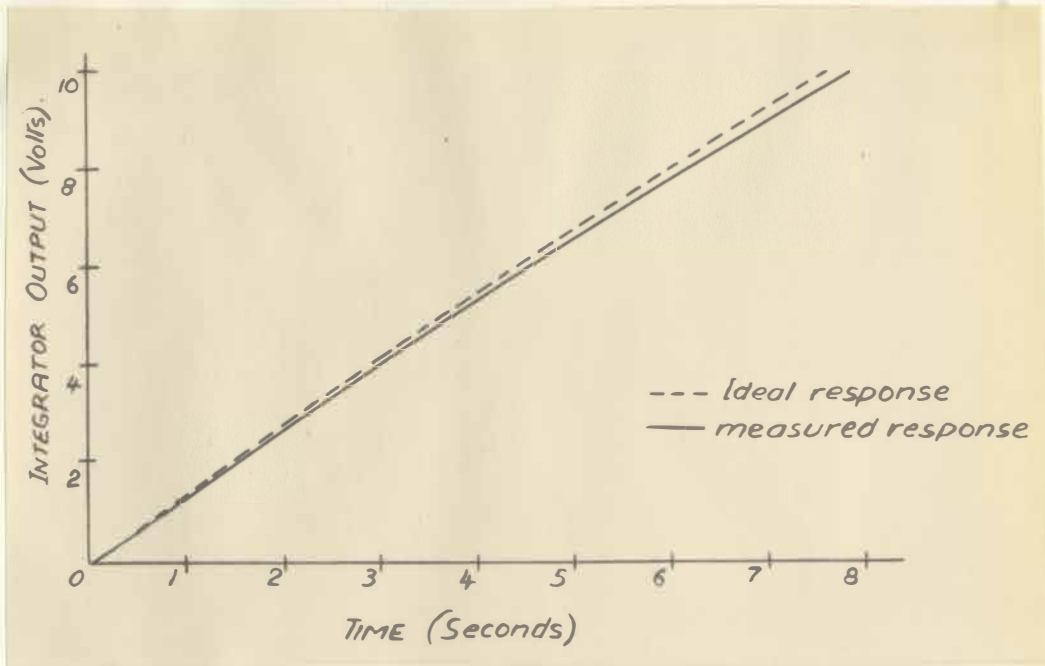


fig.4.7. Integrator response to a step input.

The value of the feedback capacitor C was chosen to be bigger than the value used in obtaining the swing curves shown in section 4.2. This was done to ensure that there would be no error in the experimental results due to the limited high-frequency response of the pen recorder used to record the output of the integrator.

More detailed information of the operational amplifiers used in the generator simulator is given in ref.35. The deviation of the measured response from the ideal is caused by the finite gain of the d.c. operational amplifier. ³²

5. CONCLUSIONS.

The simulator described is a laboratory model built to investigate a different method of coupling a d.c. analogue of a generator to an a.c. network analyser. The results obtained show that it is feasible to control the frequency of an oscillator in accordance with the generator swing equation, instead of the phase of a master oscillator feeding all the machine units in a network analyser.^{20, 22, 23, 25.}

Although the experimental swing curves are compared with calculated curves for which zero damping had been assumed, the effect of damping on the measured results is as expected. Damping reduces the amplitude of the internal angle swing, as well as the swing period (especially when the internal angle approaches the critical value, beyond which synchronism is lost).

A governor analogue can be added by building a circuit which controls the reference voltage V_r (see fig.3.1 p.10) in accordance with the governor characteristic.

The effects of variation in excitation and the action of a voltage regulator can be included by adding a circuit which will both change the amplitude of the internal emf. (power amplifier output voltage) and the amplitude of the electrical power (voltage fed back from the phase detector to the integrator). This can be done by adjusting the gain of the pre-amplifier (fig.E7, appendix E) and the gain of the d.c. amplifier in the feedback path (fig.E3, appendix E) in conjunction.

After.....

After these additional units have been added, it should be possible to study the asynchronous performance of a generator. E.g. load rejection tests could be done.

The accuracy of the simulator can be improved by using a better operational amplifier in the integrator circuit. As shown in fig.4.7, there is an error due to the finite gain of the amplifier. To reduce this error an increase in amplifier gain is required. However, the increase in amplifier complexity to reduce the error by an order of magnitude may offset the advantage of greater accuracy.

The major drawback of this simulator, and of all hybrid simulators, is that it is difficult to make the internal impedance of the generator, which appears in the a.c. part of the circuit, change. A real generator's internal impedance changes from its steady-state value to some transient value during a disturbance. It might, however, be possible to control the power amplifier/^{output}amplitude and phase in such a fashion that a variable emf. behind a fixed impedance appears like an emf. behind a variable impedance.

As with other simulators of this type, once the networks between machines have been reduced to their equivalent single phase circuits, the time required to set up, operate and obtain results is very short. Changes in machine constants can easily be made, and their effect on the behaviour of the generator observed.

With further development this simulator should be of use in the investigation of the performance of generators and their ancilliary equipment. A number of these units can be used to study multi-machine problems.

APPENDIX A

Generator damping

The expression for the damping power ³⁰ in a machine is given as:

$$P_d = V^2 \omega \left[\frac{x'_d - x''_d}{(x_e + x'_d)^2} \cdot T''_{do} \sin^2 \delta + \frac{x'_q - x''_q}{(x_e + x'_q)^2} \cdot T''_{qo} \cos^2 \delta \right] \quad (A1)$$

where P_d = instantaneous damping power, per-unit

V = voltage of infinite busbar, per-unit

s = slip, per-unit see equation A2

$\omega = 2\pi \cdot$ rated frequency, rad. per sec.

x'_d, x''_d, x'_q, x''_q = machine reactances, per-unit

x_e = external reactance in series with the armature, per-unit.

T''_{do}, T''_{qo} = open circuit direct-axis and quadrature-axis subtransient time constants, seconds.

δ = angle by which the generator internal emf. leads the infinite busbar voltage, electrical degrees.

The slip is defined as:

$$s = \frac{1}{360f} \cdot \frac{d\delta}{dt}$$

where f = rated frequency c/s

Substituting equation A2 in A1:

$$P_d = V^2 \left[\frac{x'_d - x''_d}{(x_e + x'_d)^2} \cdot T''_{do} \sin^2 \delta + \frac{x'_q - x''_q}{(x_e + x'_q)^2} \cdot T''_{qo} \cos^2 \delta \right] 2 \cdot \pi \cdot f \cdot \frac{1}{360f} \cdot \frac{d\delta}{dt}$$

$$= V^2 \left[\frac{x'_d - x''_d}{(x_e + x'_d)^2} \cdot T''_{do} \cdot \sin^2 \delta + \frac{x'_q - x''_q}{(x_e + x'_q)^2} \cdot T''_{qo} \cos^2 \delta \right] \frac{\pi}{180} \cdot \frac{d\delta}{dt}$$

defining the 'damping coefficient' K_d as:

$$K_d = \frac{P_d}{\frac{d\delta}{dt}} \quad \text{KW sec per el.degr./KVA}$$

$$\text{i.e. } K_d = V^2 \frac{\pi}{180} \left[\frac{x_d' - x_d''}{(x_e + x_d)^2} \cdot T_{do}'' \cdot \sin^2 \delta + \frac{x_q' - x_q''}{(x_e + x_q)^2} \cdot T_{qo}'' \cos^2 \delta \right] \quad (A3)$$

equation A3 is of the form:

$$K_d = V^2 \frac{\pi}{180} (a \cdot \sin^2 \delta + b \cdot \cos^2 \delta) \quad \text{see ref. 31.}$$

the average value of K_d is:

$$\begin{aligned} K_{d(av.)} &\approx V^2 \frac{\pi}{180} \cdot \frac{a + b}{2} \\ &= V^2 \frac{\pi}{360} \left[\frac{x_d' - x_d''}{(x_e + x_d)^2} \cdot T_{do}'' + \frac{x_q' - x_q''}{(x_e + x_q)^2} \cdot T_{qo}'' \right] \end{aligned} \quad (A4)$$

$$\text{But } T_d'' = \frac{x_d''}{x_d'} \cdot T_{do}'' \quad (A5)$$

where T_d'' = short-circuit direct axis subtransient time constant, sec.

$$\text{Similarly } T_q'' = \frac{x_q''}{x_q'} \cdot T_{qo}'' \quad (A6)$$

Expressing $K_{d(av.)}$ in terms of T_d'' and T_q'' , x_e disappears, since the external reactance in series with the armature is zero when the armature is short circuited.

Substituting equations A5 and A6 in A4:

$$K_{d(av.)} = V^2 \frac{\pi}{360} \left[\left(\frac{1}{x_d''} - \frac{1}{x_d'} \right) T_d'' + \left(\frac{1}{x_q''} - \frac{1}{x_q'} \right) T_q'' \right]$$

This is the expression that is used to calculate K_d in the swing equation (equation 2.3-2 page 8) although as it is expressed here, it is a per-unit value.

APPENDIX B

The Phase Detector

The circuit diagram of a simple phase detector is shown in figure B1, and the vector diagram that applies to this circuit in figure B2.

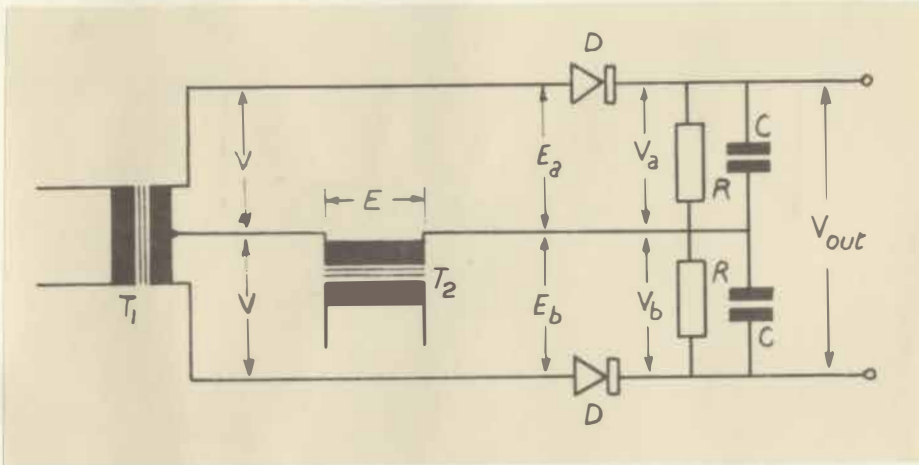


fig. B1. Basic phase detector circuit.

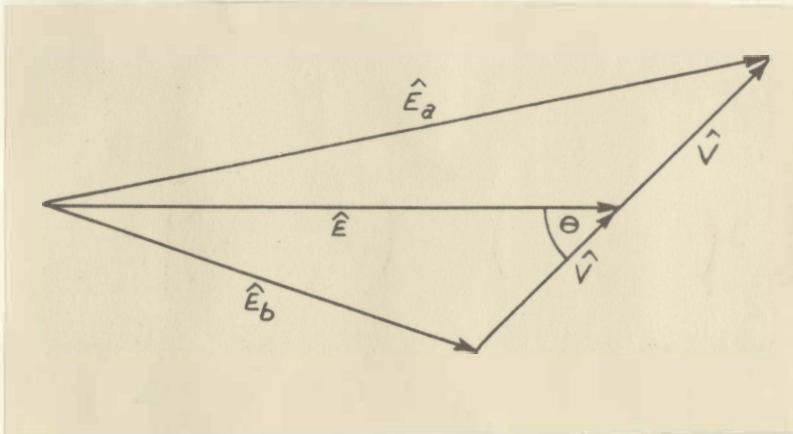


fig. B2 Vector diagram of the basic phase detector.

Referring to figures B.1 and B.2, let the secondary voltage of transformers T_1 and T_2 be $2V$ and E respectively, where

$$E = \hat{E} \sin \omega t$$

$$V = \hat{V} \sin (\omega t + \theta)$$

The voltages \hat{E}_a and \hat{E}_b which are applied to the balanced rectifier consisting of diodes D , resistors R and capacitors C are the vector sum and vector difference respectively of \hat{E} and \hat{V} . Voltages \hat{E}_a and \hat{E}_b are peak rectified, and their difference is the d.c. output voltage V_{out} .

From the vector diagram it can be seen that:

$$\hat{E}_a^2 = \hat{E}^2 + \hat{V}^2 + 2 \hat{E} \hat{V} \cos \theta$$

$$\text{and } \hat{E}_b^2 = \hat{E}^2 + \hat{V}^2 - 2 \hat{E} \hat{V} \cos \theta$$

$$\text{Now } \hat{E}_a^2 = \hat{E}^2 \left(1 + \frac{\hat{V}^2}{\hat{E}^2} + 2 \cdot \frac{\hat{V}}{\hat{E}} \cos \theta \right)$$

$$\approx \hat{E}^2 \left(1 + \frac{\hat{V}}{\hat{E}} \cos \theta \right) \text{ for } \hat{E} \gg \hat{V}$$

$$\text{i.e. } \hat{E}_a = \hat{E} \left(1 + 2 \cdot \frac{\hat{V}}{\hat{E}} \cdot \cos \theta \right)^{\frac{1}{2}}$$

expanding this gives:

$$\hat{E}_a = \hat{E} \left(1 + \frac{1}{2} \cdot 2 \frac{\hat{V}}{\hat{E}} \cos \theta + \dots \right)$$

$$\text{i.e. } \hat{E}_a \approx \hat{E} + \hat{V} \cdot \cos \theta \quad \text{for } \hat{E} \gg \hat{V}$$

Similarly $\hat{E}_b \approx \hat{E} - \hat{V} \cdot \cos \theta$

The output voltage is given by:

$$V_{out} = \hat{E}_a - \hat{E}_b$$

$$\approx 2 \hat{V} \cos \theta$$

$$= 2 \cdot \sqrt{2} V \cos \theta$$

where V = the r.m.s. value of \hat{V} .

If the smoothing capacitors C (see fig.B1) are left out, the output consists of the difference between two half-wave rectified sine waves, as shown in fig.B3.

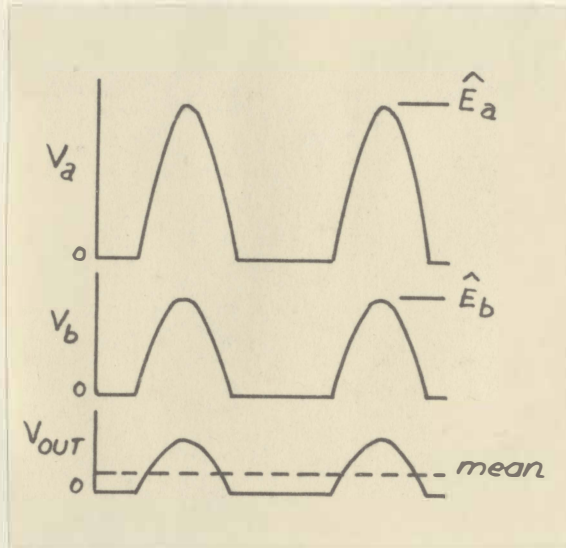


fig.B.3. Unsmoothed phase detector output.

The mean value of the output voltage now is:

$$V_{out} = \frac{1}{\pi} \cdot 2\sqrt{2} V \cos \theta \quad (B1)$$

In the interest of a quick response to an input signal, no smoothing capacitors were used in the phase detector in the generator simulator. The pulsating d.c. output voltage is adequately smoothed by the integrator, so that no pulses reach the modulator.

If we make V (Eqn. B1) proportional to the power amplifier output current I' , and θ equal to $(\delta + \phi)$ the phase angle between I' and the power

amplifier.....

amplifier output voltage (Eqn.3.1-4. p.11) the phase detector output will be a measure of the power output of the amplifier. This will only be correct if the amplifier output voltage does not fluctuate appreciably.

The circuit diagram of the phase detector, as it is connected in the generator simulator, is shown in fig. B4.

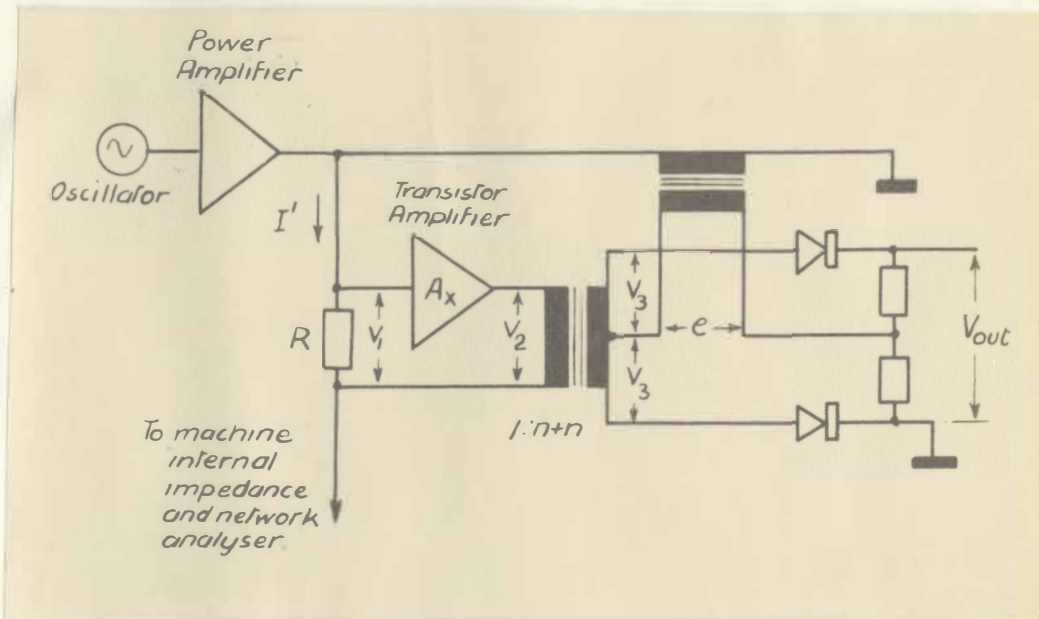


fig. B4. Phase detector connection diagram.

The output voltage of the power amplifier shown in fig. B.4 represents the internal emf. of the generator. When the simulator is connected to the network analyser, a load current I' flows from the power amplifier through series resistor R to the network analyser. The voltage v_1 developed across the resistor R is proportional to the current I' . v_1 is amplified by a transistor amplifier with voltage gain A_x . The output of the transistor amplifier is applied to the phase detector input.

The.....

The output voltage of the power amplifier is also fed to the phase detector to provide a reference voltage. The phase detector output voltage is a function of the transistor amplifier output and the phase angle ($\delta+\phi$) between the power amplifier output and the transistor amplifier output.

The output of the phase detector is related to the load current I' as shown below:

$$\begin{aligned} I' &= \text{rms. load current} \\ v_1 &= R \cdot I' \\ v_2 &= A_x \cdot v_1 \\ &= A_x \cdot R \cdot I' \\ v_3 &= n \cdot v_2 \\ &= n \cdot A_x \cdot R \cdot I' \\ V_{\text{out}} &= \frac{1}{\pi} \cdot 2\sqrt{2} \cdot v_3 \cdot \cos(\delta+\phi) \quad (\text{see equation B.1.}) \\ &= \frac{1}{\pi} \cdot 2\sqrt{2} \cdot n \cdot A_x \cdot R \cdot I' \cdot \cos(\delta+\phi) \\ &= k_\phi \cdot I' \cdot \cos(\delta+\phi) \quad (\text{see equation 3.1-4 p.11}) \end{aligned}$$

Using the constants of the circuit that had been built to calculate k_ϕ gives:

$$\begin{aligned} k_\phi &= \frac{1}{\pi} \cdot 2\sqrt{2} \cdot \frac{1}{3.4} \cdot 48 \cdot 1 \quad (\text{see appendix E section 2.1(iv)}) \\ &= 12.7 \cdot 10^{-3} \quad \text{V d.c./mA r.m.s.} \end{aligned}$$

APPENDIX C

1. Gain of the differential operational amplifier

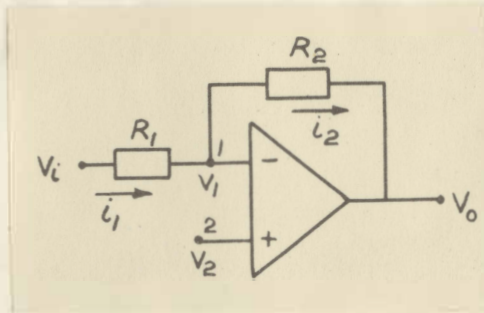


fig.C1. Differential operational amplifier.

Consider the amplifier shown in fig.C1. Let its gain be A. At input terminal 1, neglecting the grid current:

$$i_1 = i_2 \quad (\text{see ref. 32})$$

From Ohm's law and the above identity

$$\frac{V_i - V_1}{R_1} = \frac{V_1 - V_o}{R_2} \quad (C1)$$

also $\frac{V_o}{A} = V_2 - V_1 \quad (C2)$

Eliminating V_1 by substituting equation C2 in equation C1, and solving for V_o gives:

$$V_o = \left[\frac{R_1 + R_2}{R_1} \cdot V_2 - \frac{R_2}{R_1} \cdot V_i \right] \frac{1}{1 + \frac{R_1 + R_2}{A \cdot R_1}}$$

if $A \gg 1$, $V_o = \frac{R_1 + R_2}{R_1} \cdot V_2 - \frac{R_2}{R_1} \cdot V_i \quad (C3)$

note: there is no phase reversal between V_o and V_2 .

2. The damped integrator

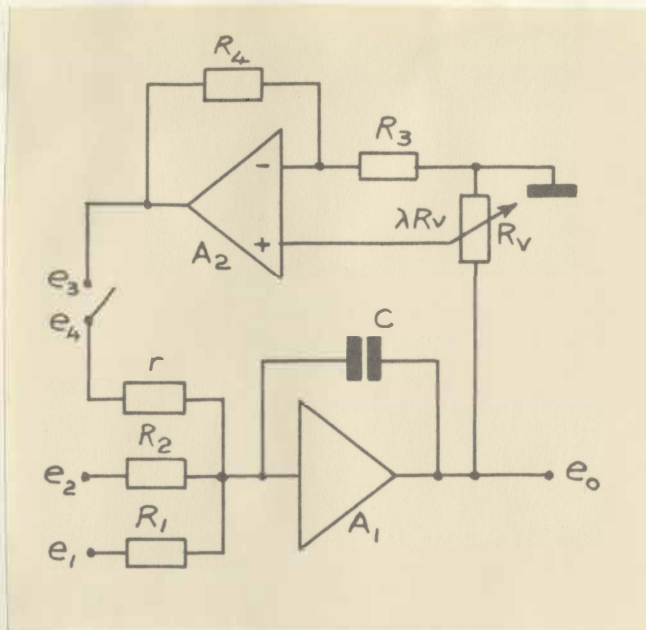


fig. C2_ Integrator with damping loop.

The usual assumptions made for an operational amplifier are made, i.e. the gain of the amplifier is very much greater than unity, and grid current is negligible.

The output voltage e_o of the circuit shown in fig. C2 is given by:

$$- e_o = \frac{1}{R_2 C} \int e_2 \cdot dt + \frac{1}{R_1 C} \int e_1 \cdot dt + \frac{1}{r C} \int e_3 \cdot dt$$

$$\text{let } R_1 = R_2 = R$$

$$\text{now } - e_o = \frac{1}{RC} \int (e_1 + e_2 + \frac{R}{r} \cdot e_3) dt. \quad (C4)$$

The output of amplifier A_2 is:

$$e_4 = \lambda \cdot \frac{R_2 + R_4}{R_3} \cdot e_o$$

$$= 2 \cdot \lambda \cdot e_o \text{ for } R_3 = R_4$$

Closing.....

Closing switch S makes $e_3 = e_4$. Substituting the expression for e_4 in equation C4 gives:

$$-e_o = \frac{1}{RC} \int (e_1 + e_2 + \frac{R}{r} \cdot 2.\lambda.e_o) dt.$$

This expression is identical to equation 3.2-17, where:

$$v_4 = -e_o$$

$$v_r = e_1$$

$$v_2 = e_2$$

Appendix D Alternator damping coefficient

1. Machines described in Study 1

Equation A7 in appendix A gives the damping coefficient of a generator as being:

$$K_d = V^2 \cdot \frac{\pi}{360} \left[\left(\frac{1}{x_d''} - \frac{1}{x_d'} \right) T_d'' + \left(\frac{1}{x_q''} - \frac{1}{x_q'} \right) T_q'' \right]$$

where $T_d'' = \frac{x_d''}{x_d'} \cdot T_{do}''$ and $T_q'' = \frac{x_q''}{x_q'} \cdot T_{qo}''$

The machines in problem 1 are 30 MVA waterwheel generators.

Ref.30 (p.218 table 3 and p.240, example 2) gives figures which were taken as being typical for a machine of this type and rating. The following figures were taken from ref.30.

Reactances in per-unit :

$$x_d' = 0.37 \qquad x_d'' = 0.24$$

$$x_q' = 0.75 \qquad x_q'' = 0.34$$

Time constants in seconds :

$$T_{do}'' = 0.035 \qquad T_{qo}'' = 0.035$$

Let $V = 0.95$ per unit (as given in section 4.2.1.)

= infinite busbar voltage.

Substituting the figures in the expression for the damping coefficient gives:

$$K_d = 4.7 \cdot 10^{-4} \text{ KW sec/KVA degree.}$$

Equation 3.3-4 p.22 gives an expression for the damping coefficient

K_d' of the generator simulator, which is:

$$K'_d = \frac{2 \cdot \lambda \cdot R \cdot E'_r \cdot E_{p.u.} \cdot P}{\alpha \cdot k_m \cdot r \cdot k \cdot P'}$$

The swing curves shown in fig. 4.4. were taken with the following values for the symbols in the above expression: (see section 4.2.1.)

$$\lambda = 0.29 \quad (\text{see fig. 3.3. page 20})$$

$$R = 120 \text{ K.ohm}$$

$$E'_r = 10V$$

$$E_{p.u.} = 1.125 \text{ p.u.}$$

$$P = 60 \text{ MVA}$$

$$\alpha = 0.12$$

$$k_m = 12.18 \text{ rad. per. sec/V}$$

$$r = 1 \text{ M.ohm}$$

$$k = 0.254 \text{ V/mA}$$

$$P' = 100 \text{ mVA}$$

Using the above figures gives K'_d a value of

$$\begin{aligned} K'_d &= 1.27 \cdot 10^6 \text{ W sec/rad.} \\ &= 22.2 \cdot 10^3 \text{ W sec/degr.} \end{aligned}$$

On a base of 60 MVA, the per-unit damping coefficient is:

$$K'_d = 3.7 \cdot 10^{-4} \text{ KW sec/KVA degr.}$$

Comparing the damping coefficients of the generator and the simulator shows that there is less damping in the simulator than the figure assumed for the equivalent generator in the problem. If the generator damping coefficient were given, the simulator damping coefficient could be set to that value since the minimum simulator damping coefficient would be less than the generator damping coefficient.

2. Damping coefficient - Study 2

The generator mentioned in Section 4.2.2 is a 25 MVA waterwheel machine. Since its reactances and time constants are not given, it is assumed that the figures given in section 1 of appendix D are typical of a machine of this rating.

Calculating the damping coefficient as before, and using a voltage of 1.00 p.u. as the infinite busbar voltage (see section 4.2.2) gives K_d as being:

$$K_d = 5.2 \cdot 10^{-4} \text{ KW sec/KVA degr.}$$

For calculating K_d^1 all constants are the same as in page D2, except for the following:

$$E_{\text{p.u.}} = 1.03 \text{ per unit}$$

$$P = 25 \text{ MVA}$$

using these figures gives:

$$K_d^1 = 7.6 \cdot 10^{-4} \text{ KW sec/KVA degree on a base of 25 MVA.}$$

The damping coefficient of the simulator cannot be reduced below the equivalent of 22.2 KW sec/deg. Further reduction in K_d^1 causes the simulator to start hunting.

Regarding the simulator as a feedback control loop, it can be said that the device will be unstable if the phase shift around the loop reaches 180° whilst the loop gain is still greater or equal to unity.

In this apparatus the integrator causes a 90° phase shift. Any other 90° phase shift in the same sense will thus lead to instability. Such an additional phase shift is produced by the low pass filter following the variable frequency oscillator, as shown in fig.E8.

A phase-lead network could be put in the feedback loop to reduce the loop phase shift, but since the frequency of hunting is also the frequency at which the simulator oscillates during transient studies, such a network would not only affect the hunting but also influence the transient performance of the simulator.

It appears as if the problem can be solved by putting a lead network in circuit after the filter. This network could be a single-stage pentode connected as a differentiator, as shown below:

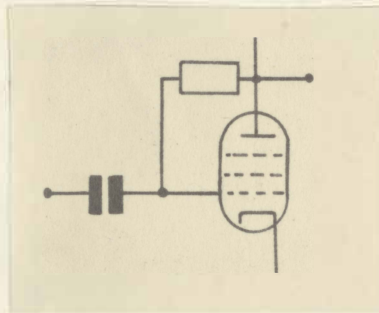


fig.D1. Phase compensating element.

This circuit will cause a phase shift in the oscillator output which will cancel the phase shift produced by the filter.

In this part of the loop a phase shift will not affect the d.c. analogue, but it should make it possible to reduce the damping to a value equal to the damping of a generator.

Appendix E

Specifications and circuit diagrams of the units comprising the generator simulator.

The simulator can be split into two sections, i.e. a part consisting of the d.c. analogue circuit, and a section which includes the coupling units and the a.c. units, as shown in fig. E.1.

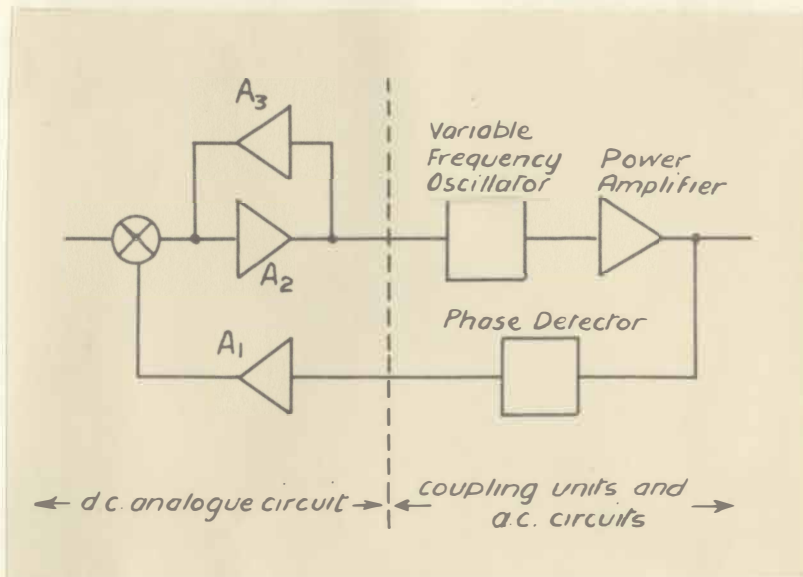


fig. E.1. Block diagram of the generator simulator.

1. D.C. AMPLIFIERS

The d.c. analogue circuit contains three d.c. operational amplifiers, which are identical to those designed for the computer described in ref.35. The theory of their feedback circuitry is explained in appendix C.

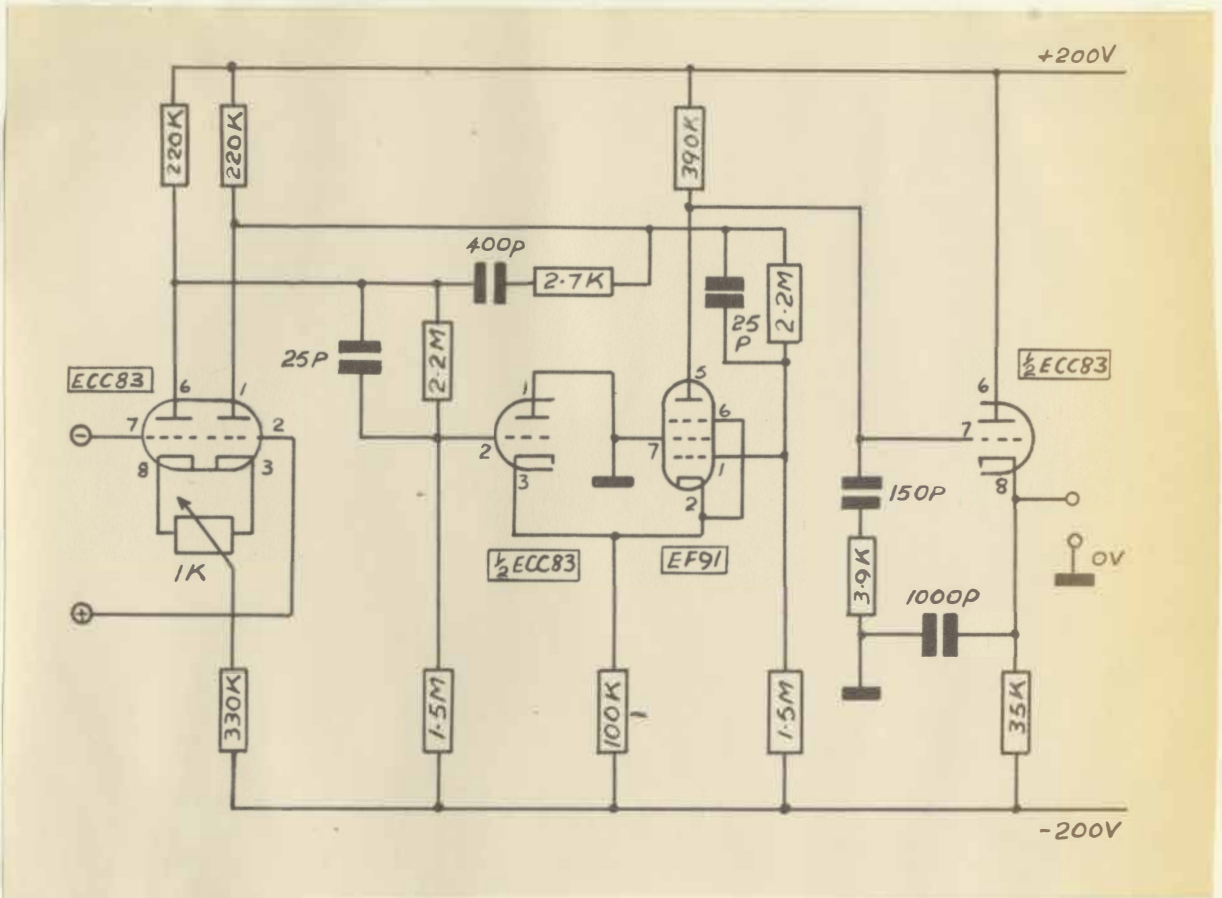


Fig. E.2. D.c. operational amplifier.

Specifications of the d.c. amplifier:

Gain = 6,700

Bandwidth = dc to 5 Kc/s (-3dB)

Max.output = \pm 40 V

Max.load = 30 K.ohm.

Further information on the d.c. amplifier is given in ref. 35.

Feedback.....

Feedback loop d.c. amplifier A_1

The amplifier in the feedback loop of the simulator has its feedback resistors connected as shown in fig. E.3.

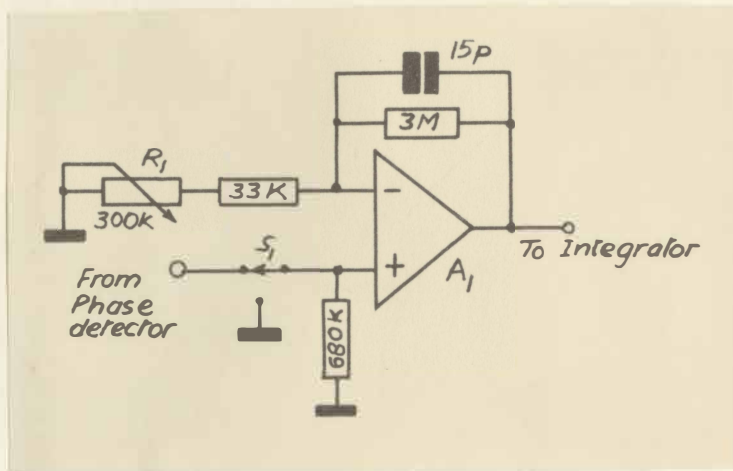


Fig.E.3. Connection diagram of amplifier in simulator feedback loop.

Switch S_1 allows the amplifier input to be earthed, so that the d.c. balance of the d.c. amplifier A_1 can be adjusted. Variable resistor R_1 controls the gain of the amplifier, and thus the constant k (see equation 3.1-5 p.11). Changing k is equivalent to changing the excitation of a generator as far as the d.c. analogue is concerned.

Integrator.....

Integrator and damping amplifier

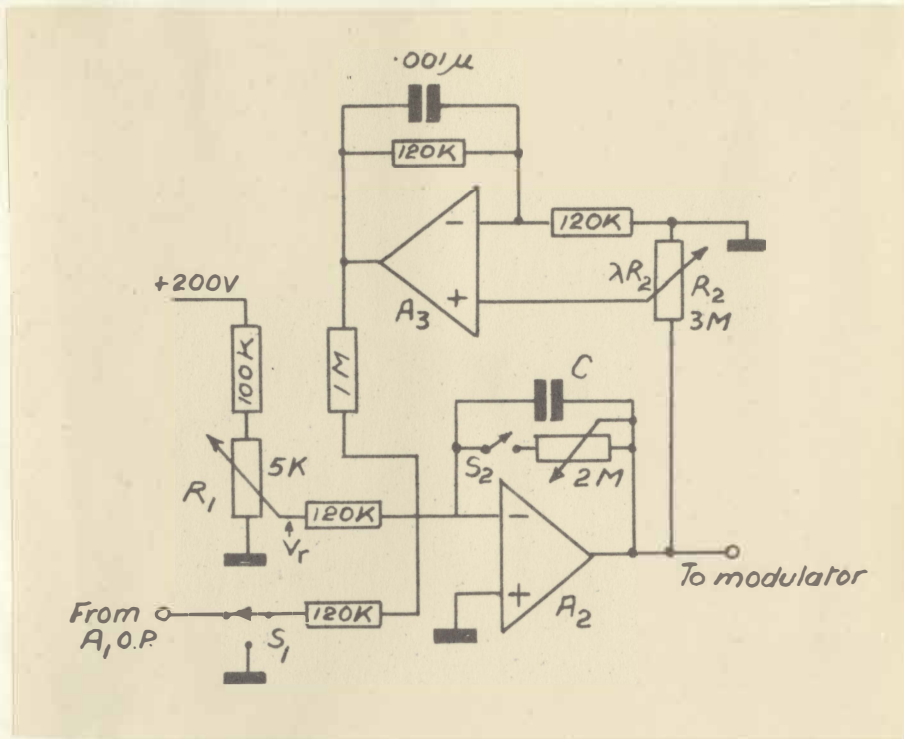


Fig.E.4. Integrator and damping amplifier connection diagram.

S_1 earths the integrator input when amplifier A_2 is being balanced.

S_2 connects a resistor across the feedback capacitor of the integrator amplifier A_2 to make balancing easier,

R_1 controls the voltage that backs off the feedback signal from the phase detector and its d.c. amplifier. This voltage, V_r , is the equivalent of the mechanical power input to the generator. R_1 thus is the "steam valve".

R_2 determines the amount of damping of the integrator. When the full output of the integrator is fed to the damping amplifier A_3 , $\lambda = 1$ (see equation 3.3-4, e.g.)

C is the feedback capacitor of the integrator. Changing C is equivalent to changing the inertia constant of a generator.

2. A.C. units. The a.c. section of the simulator consists of a variable frequency oscillator, a filter and pre-amplifier, a power amplifier and a phase detector.

(i) Variable frequency oscillator

Although a separate modulator and oscillator were shown in the block diagram (fig.3.1. p 10) the two units are in fact combined in one circuit.

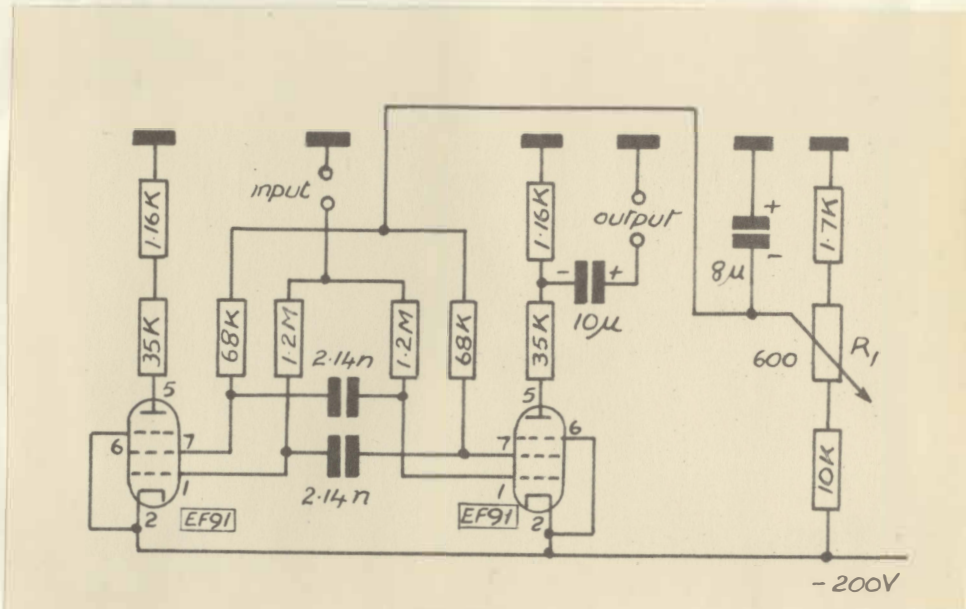


fig. E.5. Variable frequency oscillator.

A multivibrator oscillator was used, since the amplitude of its output voltage is independent of all except the supply voltage, and that can be stabilised easily. Potentiometer R_1 , sets the frequency of oscillation. The frequency is controlled by applying a voltage to the input terminals.

The.....

The characteristic of the oscillator is shown in fig. E.6.

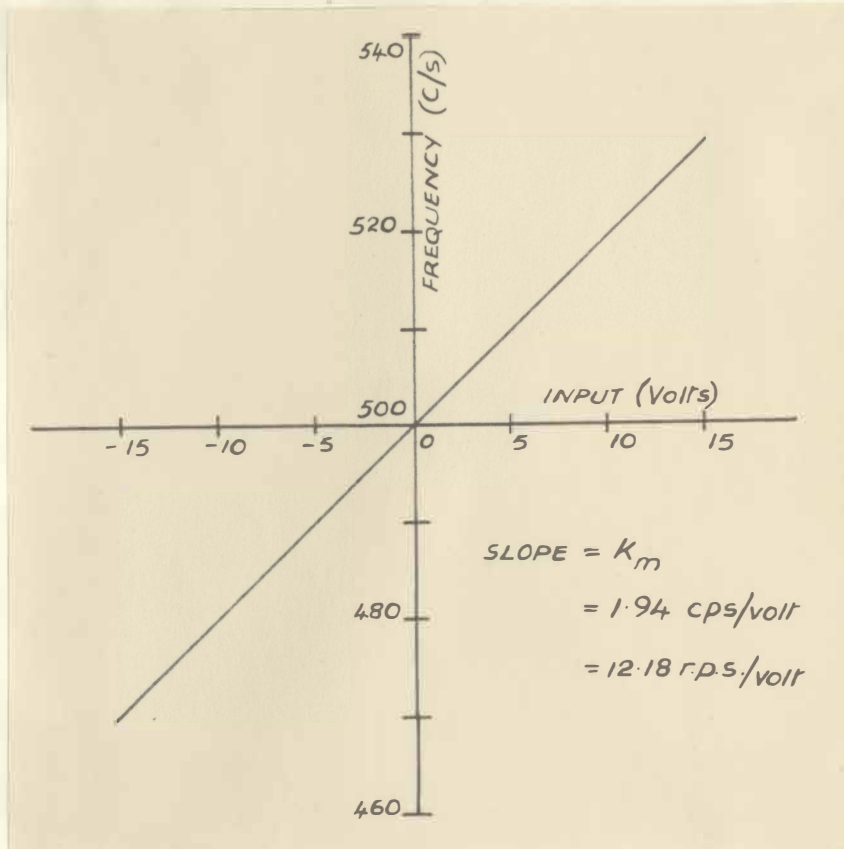


Fig. E.6. Oscillator frequency vs. input voltage.

(ii) Low-pass filter and pre-amplifier

The square wave output of the oscillator is passed through a low-pass filter and amplified by a pre-amplifier, where the amplitude of the signal can be adjusted.

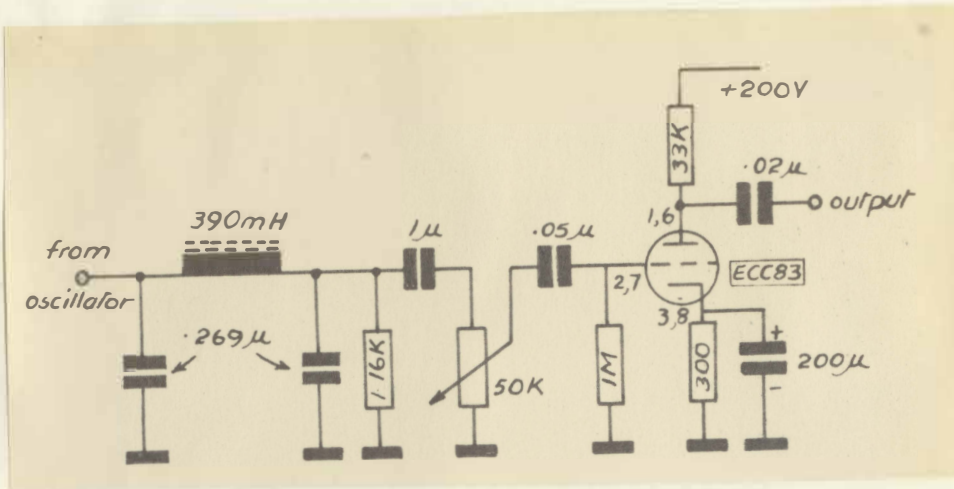


Fig. E.7. Low-pass filter and pre-amplifier.

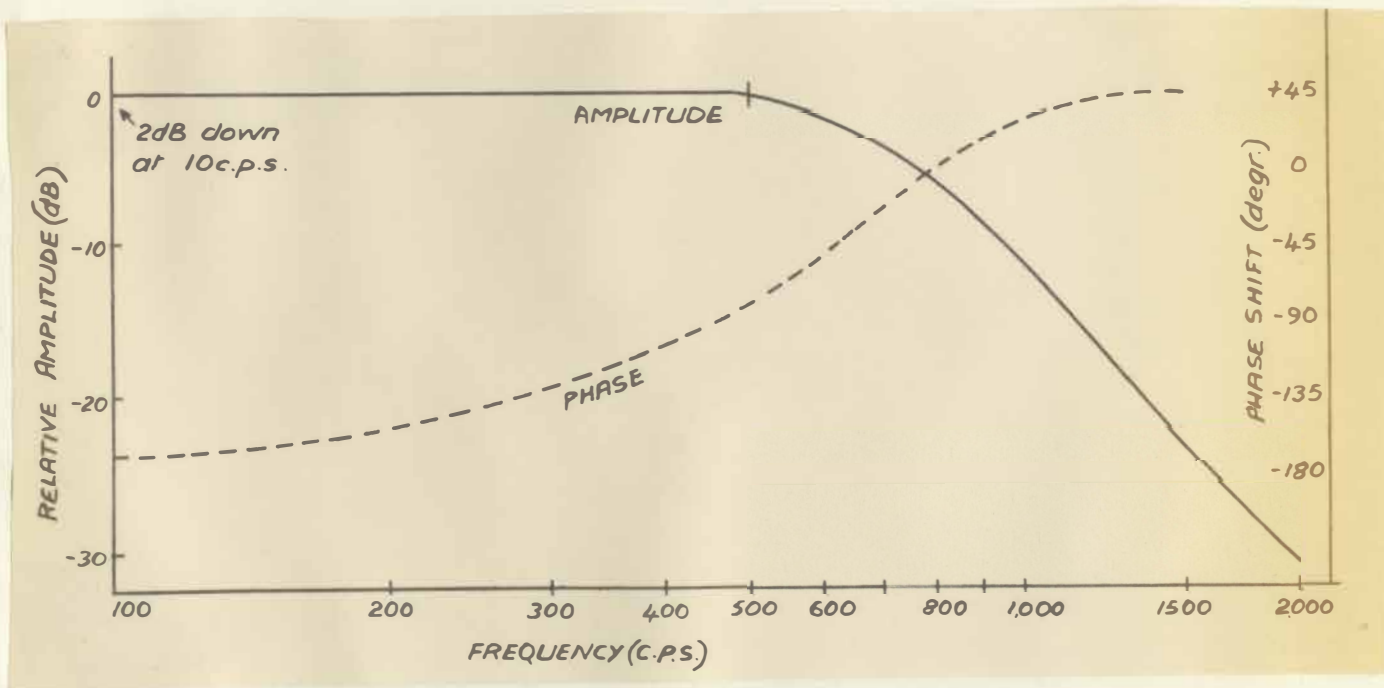


Fig.E.8. Frequency response curves of low-pass filter and preamplifier.

Amplifier.....

Amplifier gain = 34 dB (measured at 500 c/s)

Filter attenuation = 8 dB in pass band (measured at 500 c/s). The third harmonic of the fundamental is a third of the amplitude of the fundamental in a perfect square wave. The filter reduces the third harmonic of the square wave input by another 20 dB, so that the output of the filter is a sine wave with very little distortion (about 3%).

(iii) Power amplifier

The output from the pre-amplifier shown in fig.E.7 is passed through an amplifier to obtain a low impedance source for feeding the network analyser. The amplifier must be able to feed sufficient current into resistive and reactive loads such as the impedances in the network analyser require.

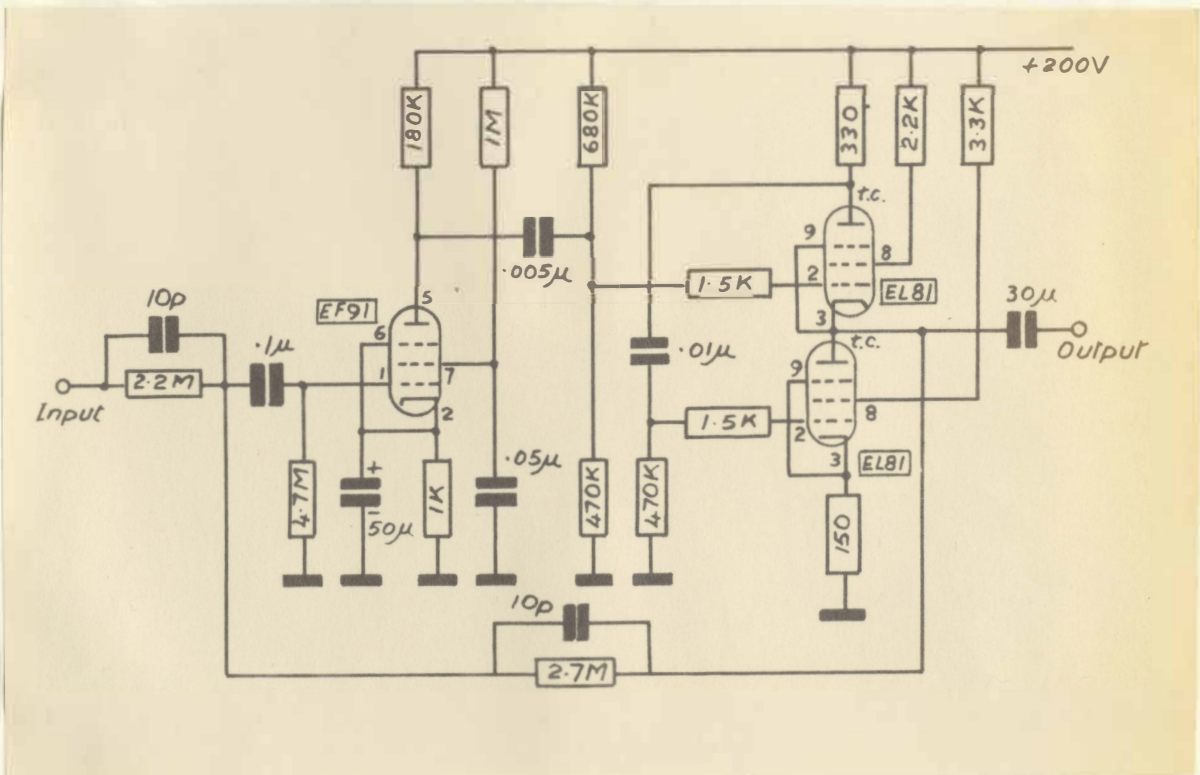


Fig.E.9. Power amplifier.

Power amplifier specifications:

Without feedback:

gain = 45 dB at 500 c/s

output impedance = 45 ohms.

With feedback:

gain = 1.1 dB

output impedance = 0.5 ohms.

Bandwidth : 15 c/s to 50 kc/s (-1dB)

(iv) Phase detector (see appendix B)

Instead of using a current transformer to obtain a voltage proportional to the output current of the phase detector, a low value resistor was put in series with the power amplifier. The voltage drop across this series resistor is amplified by a floating transistor amplifier (fig. E.10) whose output is applied to the phase detector proper (fig. E.11).

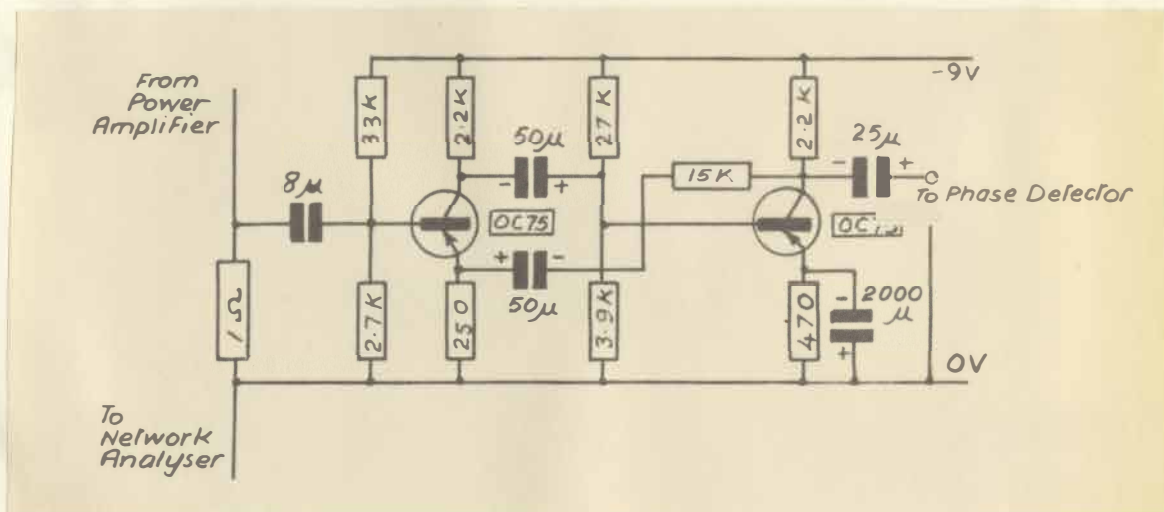


Fig. E.10 Transistor amplifier.

Transistor.....

Transistor amplifier specifications.

With feedback, and with load connected:

Gain = 48

Bandwidth : 12 c/s to 100 Kc/s (-3dB)

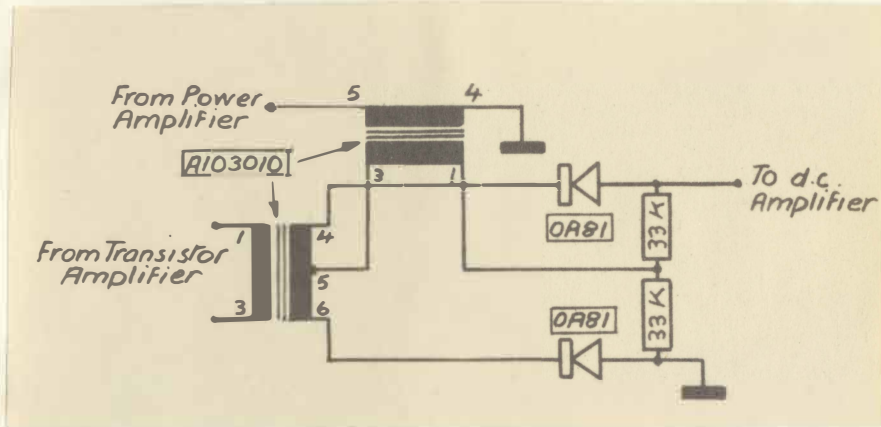


Fig. E.11 Phase detector.

Appendix F Auxilliary equipment

1. Phase angle recorder

An instrument had been built³³ which could measure the phase angle between two 500 c/s voltages. It is used in the simulator to measure the angle between the generator internal emf. (power amplifier output voltage) and infinite busbars (reference voltage in the network analyser).

The relative phase angle of the two voltages is measured by squaring and differentiating the two signals to get two series of pulses, which occur at the instants where the two input voltage sinusoids are zero. These pulses are then shaped in two monostable multivibrators. The one series of pulses is used to synchronise a saw-tooth generator. The other series of pulses switches a sampling circuit, which samples the height of the saw-tooth voltage once per cycle. The sampling circuit stores the voltage it measures for one cycle, when

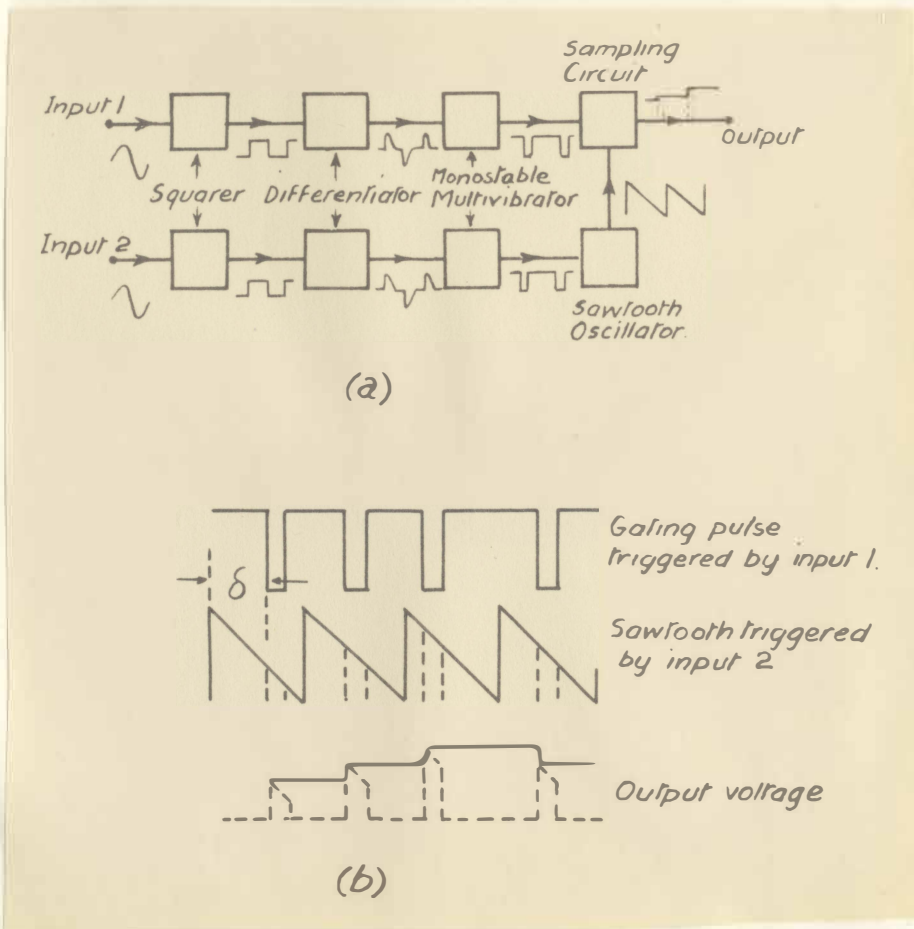


Fig.F.1. Phase angle recorder. (a) Block diagram. (b) Waveforms.

it repeats its measurement. The voltage in the sampling circuit, which is a measure of the phase angle between the two voltages, can be displayed on a C.R.O. (for transient measurements) or a high resistance d.c. voltmeter.

2) Network impedance switching unit

A switch was built³⁶ which made it possible to apply and clear faults in the network between the generator simulator and the reference oscillator in the network analyser. The fault duration can be set to the required time, and provision is made for the post-fault impedance to be either more or less than the pre-fault impedance.

The unit consists of a 1000c/s clock oscillator followed by a pulse shaping circuit to convert the oscillator output into pulses. The pulses are used to drive two cold cathode decade scaling tubes. By making a connection to the appropriate cathodes of the scaling tubes, pulses with a spacing of 1 to 900 m.sec. can be obtained.

The output from the scaling tubes is used to drive a bistable circuit, which operates a number of high speed change-over relays. The relays go from one position to another for the period of time between the pulses from the scaling tubes. By making appropriate connections to the relays, the desired switching operations can be obtained.

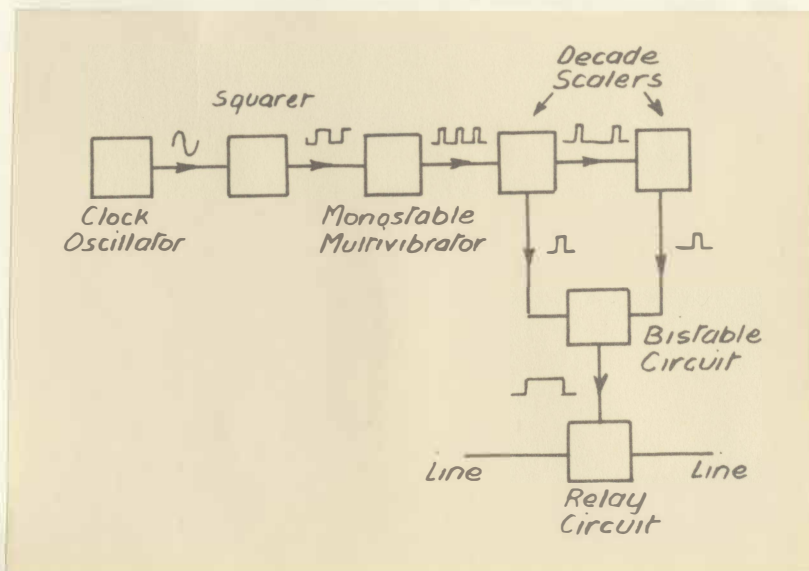


Fig. F.2. Switch unit.

REFERENCES

1. Horsley, W.D.: 'Turbo-type generators. Review of progress', Proc. IEE, 1963, 110, p.695-696.
2. Scott, E.C., Casson, W., Chorlton, A., Banks, J.H. 'Multi-generator transient-stability performance under fault conditions', Proc. IEE, 1963, 110, p.1051.
3. Laible, Th.: 'The reactances and other constants of the synchronous machine', Bulletin Oerlikon, 1954, Vol.XXXIII No.300, p.68.
4. Say, M.G., 'Power System Analysers and Computers'- Micro-networks of the USSR', Electrical Journal CLXVIII No. 9, 1962, p.494.
5. Chorlton, A., Robert, R., Concordia, C., 'Computational aids to power system analysis', C.I.G.R.E. 1954, paper No. 323.
6. Sudan, R.N., Manohar, V.N., Adkins, B., 'The measurement of transient torque and load angle in model synchronous machines', Proc. IEE, 1960, 107 A, p.51.
7. Buehler, H., 'Theory of design of an improved electronic generator model', Bulletin Oerlikon, 1958, No. 330, p. 120.
8. Kaneff, S., 'Dynamic operation of an a.c. network analyser', Proc.IEE, 1955, 102 A, p. 597.
9. Adamson, C., Barnes, L., Nellist, B.D. 'The automatic solution of power-system swing curves', Proc. IEE, 1957, 104 A, p. 143.
10. John, M.N.: 'A general method of digital network analysis particularly suitable for use with low-speed computers', Proc.IEE, 1961, 108 A, p.369.
11. Gupta, P.P., Humphrey Davies M.W: 'Digital computers in power system analysis', Proc. IEE, 1961, 108 A, p.369.
12. Brown, R.J., Tinney, W.F. 'Application of digital computers in power systems analysis', C.I.G.R.E. 1958 paper No.307.
13. Shen, D.W.C., Packer, J.S.: 'Analysis of hunting phenomena in power systems by means of electrical analogues', Proc. IEE, 1954, 101 II, p.21.
14. Dineley, J.L., Glover, K.J.: 'Synchronous-generator voltage saturation', Journal IEE, 1964, Vol. 10, p.79.
15. Alfred, A.S., Shackshaft, G: 'The effect of a voltage regulator on the steady-state and transient stability of a synchronous generator', Proc. IEE, 1958, 105 A. p. 420.

16. Shackshaft, G.: 'General-purpose turbo-alternator model', Proc.IEE, 1963, 110, p.703.
17. Aldred, A.S., Doyle. P.A.: 'Electronic-analogue-computer study of synchronous-machine transient stability', Proc.IEE, 1957, 104 A. p. 152.
18. Aldred, A.S.: 'Electronic analogue computer simulation of multi-machine power-system networks', Proc.IEE, 1962, 109 A, p.195.
19. Miles, J.G.: 'Analysis of overall stability of multi-machine power systems', Proc. IEE, 1962, 109 A, p. 203.
20. Shen, D.W.C., Lisser, S.: 'An analogue computer for automatic determination of system swing curves', Trans.AIEE, 1954, Vol.73, Part I, p.475.
21. Kaneff, S.: 'A high-frequency simulator for the analysis of power systems', Proc. IEE, 1953, 100 II, p. 405.
22. Walker, P.A.W., Aldred, A.S.: 'Displacement governing in a 2-machine system - a hybrid simulator study', Proc.IEE, 1964, 111, p.325.
23. Dineley, J.L.: 'Study of power-system transient stability by a combined computer', Proc. IEE, 1964, 111, p.107.
24. Dineley, J.L., Powers, E.T.: 'Power-system governor simulation', *ibid.*p.115.
25. Corless, K.G., Aldred, A.S.: 'An experimental electronic power-system simulator', Proc. IEE. 1958, 105 A, p.503.
26. Dineley, J.L., Humpage, W.D., 'Aids in the calculation of transient stability', Journal IEE, 1962, Vol.8, p.86.
27. Say, M.G.: 'The performance and design of alternating current machines' (Pitman, 1958) p.451-453.
28. Kimbark, E.W.: 'Power system stability' Vol.1 (Wiley, 1949) p.15 - 26.
29. Crary, S.B.: 'Power system stability' Vol.2 (Wiley 1947) p.88.
30. Kimbark, E.W.: 'Power system stability' Vol.3 (Wiley, 1956) p.234.
31. Crary, S.B.: 'Power system stability' Vo. 2 (Wiley 1947) p. 152.
32. Howe, R.M.: 'Design fundamentals of analog computer components' (van nostrand 1961) p.22-24.
33. Lewis-Roberts, P.L.: 'Phase angle recorder', B.Sc.thesis No.7, 1962, Dept. of Electrical Engineering, University of Cape Town.

34. Westinghouse Electrical and Manufacturing Co.: 'Electrical transmission and distribution reference book' (1944) pp. 211-215.
35. Powell, W.H.: 'A basic analogue computer'. B.Sc.thesis No. 19, 1960, Dept. of Electrical Engineering, University of Cape Town.
36. Duminy, F.J.: 'A model transmission line switch' B.Sc.thesis No.15, 1963, Dept. of Electrical Engineering, University of Cape Town.